SYNOPTIC ASPECTS OF CYCLOGENESIS

Lance F. Bosart
Department of Atmospheric Science
State University of New York at Albany
1400 Washington Avenue
Albany, New York 12222
U.S.A.

Summary: This paper reviews the synoptic aspects of the cyclogenesis problem. It begins with a climatological overview of cyclogenesis in the Northern Hemisphere. This is followed by a brief theoretical review of synoptic principles from Sutcliffe development theory through quasi-and semi-geostrophic theory and the isentropic potential vorticity viewpoint. The paper concludes with examples of explosive cyclogenesis over North America and the North Atlantic. Physical processes which reduce the lower tropospheric large scale static stability and enhance the baroclinicity, vorticity and convergence in the presence of deep baroclinicity ahead of a migratory disturbance aloft are shown to be crucial to rapid cyclone spin-up.

1. INTRODUCTION

Modern studies of synoptic scale cyclogenesis owe their origin to the advent of numerous kite soundings and especially the operational implementation of the radiosonde. For example,

Bjerknes, Solberg, Bergeron and their collaborators used swarm radiosonde ascents to deduce much of the horizontal and vertical structure of migratory synoptic disturbances across western and central Europe. The concept of a more or less continuous polar front circling the globe in middle latitudes upon which wave cyclones evolved in accordance with the now familiar polar front model was a direct result of these endeavors. Pioneering theoretical and observational work by Charney (1947), Eady (1949) and Sutcliffe (1947), among others, has resulted in the quasi-geostrophic viewpoint to explain synoptic development centered around finite amplitude perturbations in the middle latitude westerlies.

In the opinion of this writer, however, the polar front cyclone model has grown somewhat creaky with age and should probably be abandoned. An example would be the familiar cyclone occlusion process in which the cyclone is said to occlude when the advancing cold air catches up with and undercuts the warm air. An alternative intrepretation would be that the cyclone deepens continuously into the cold air in response to cyclonic vorticity advection aloft. In this view the "occluded front" grows continuously toward colder 1000-500 mb thickness values. Quasi-geostrophic theory is consistent with this interpretation in that a deepening cyclone must be one over which the mean temperature is decreasing. A key factor limiting excessive development would be frictional processes. The newly emerging isentropic potential vorticity viewpoint (Hoskins et al., 1985) also requires that deepening cyclones be overtaken by a cold dome

of isentropic surfaces uplifted beneath an advancing positive potential vorticity anomaly aloft.

Other examples come readily to mind. The zipper lows along the Atlantic seaboard of the United States (Keshishian and Bosart, 1987) go through their life cycle without ever conforming to the classical occlusion process. Polar lows (described by Reed elsewhere in this seminar series) that form in a broad baroclinic environment of a decaying cyclone would be yet another example. It is quite likely, however, that such developments can be understood qualitatively from quasi-geostrophic theory and quantitatively from the context of isentropic potential vorticity.

2. CLIMATOLOGY

Petterssen (1956) published a winter and summer climatology of Northern Hemisphere cyclones and cyclogenesis for the forty year period ending 1939. Winter cyclones tended to form along the east sides of continents, downwind of major mountain barriers and over unfrozen inland water bodies. A similar, but less amplified pattern, was seen in summer. In many regions the maxima of cyclone frequency extended far to the northeast of the maxima of cyclogenesis, suggestive of long-lived cyclone tracks. A more modern view (see, e.g., Wallace and Blackmon, 1983) identifies maxima in the variance of global 500 mb geopotential heights with "storm tracks" when the data is filtered so as to isolate variations on synoptic time scales (typically 2-6 days). These "storm tracks" (representative of alterations of trough and

ridge conditions) were characterized by elongated variance maxima over the oceans near 45°N where baroclinic activity tended to be most intense. This interpretation is consistent with Petterssen's results showing maximum cyclone frequencies extending well east-northeastward from coastal cyclogenesis maxima.

Recent work by Wallace and colleagues (personal communication) and Dole (1987a, b) has concentrated on identifying the principal winter cyclone and anticyclone zones in the Northern Hemisphere on the basis of the variance of the horizontal momentum fluxes and vertical heat fluxes. These authors have used the terminology "baroclinic waveguide" to highlight channels of high variance which undulate around the globe. The concept is appealing because the baroclinic waveguides respond to both planetary and synoptic scale signals as modified by topography and land-sea temperature contrasts. The majority of the Petterssen findings are replicated by the modern dynamical analysis.

3. THEORETICAL CONSIDERATIONS

Theoretical concepts are discussed extensively elsewhere in this seminar series and so they will only be mentioned briefly here. Much of the physical basis for modern dynamic meteorology was recognized by Sutcliffe (1947) and Sutcliffe and Forsdyke (1950) nearly 40 years ago. Sutcliffe proposed that the development of cyclones and anticyclones could be deduced from simplified expressions that measured the relative divergence between the upper and lower troposphere. The dominant forcing terms proved

to be the advection of thermal vorticity by the thermal wind and the advection of surface vorticity by the thermal wind. Sutcliffe associated cyclone translation and deepening with the latter and former mechanisms respectively. The remarkable insights of Sutcliffe and colleagues was immediately apparent to weather map aficionadoes with an interest in scientific inquiry.

Petterssen (1956) extended Sutcliffe's research to include the role of adiabatic and diabatic heating and cooling. Both authors anticipated the development of quasi-geostrophic theory through their linkage of the hydrodynamic and thermodynamic equations in one surface development equation. Petterssen wrote that surface cyclone development can be expected whenever and wherever a region of appreciable cyclonic vorticity advection in the middle troposphere overspread a surface baroclinic zone. Experience with mid-latitude cyclogenesis events has shown that many cyclones (but by no means all cyclones) evolve in the manner envisioned by Petterssen and Sutcliffe.

The ideas of Sutcliffe, Petterssen and others are incorporated into the modern quasi-geostrophic theory as summarized by Phillips (1963), Sanders (1974) and Holton (1979). Briefly, a knowledge of the geopotential height and temperature fields throughout the middle latitude troposphere together with suitable lateral and vertical boundary conditions is sufficient to diagnose the vertical motion (omega equation) and predict the geopotential height tendency (height tendency equation; same equation as the quasi-geostrophic potential vorticity equation) for synoptic scale motions. The divergent secondary circulation

required to satisfy simultaneously the synoptic scale vorticity and thermodynamic equations served the purpose of maintaining hydrostatic and geostrophic equilibrium. In quasi-geostrophic theory the active cyclone deepening mechanism is an upward increase of cyclonic vorticity advection over the cyclone center (associated with ascent and thickness cooling) whereas cyclones tend to be steered toward regions of the maximum Laplacian of warm air advection in the lower troposphere. Quasi-geostrophic theory has proved to be very effective in giving us a qualitative appreciation of synoptic scale development although operational implementation of quasi-geostrophic models often produced weather maps that were mere caricatures of reality. Quasi-geostrophic models were soon abandoned in favor of full primitive equation models such as employed at ECMWF and elsewhere.

Trenberth (1978), Hoskins et al. (1978) and Hoskins and Pedder (1980) pointed out that the traditional quasi-geostrophic omega equation contained a term that cancelled between the two dominant terms and that misleading results could be obtained by partitioning the equation in the traditional format. Hoskins and collaborators showed that the omega equation could be recast in terms of one forcing function ($\nabla \cdot \vec{Q}$) that could be evaluated from a knowledge of the temperature and geopotential fields on an individual isobaric surface. Regions of convergence (divergence) of $\vec{Q}$ could be associated with ascent (descent) respectively. The $\vec{Q}$ -vector had the further advantage that when dotted into the horizontal gradient of potential temperature the resulting expression was proportional to the rate of quasi-geostrophic

frontogenesis.

Semi-geostrophic theory (Eliassen,1948) and Hoskins, 1975) has quantitatively improved upon quasi-geostrophic theory by allowing for advection by the full wind instead of the geostrophic wind in the presence of flow curvature. A Lagrangian time scale (long compared to the inverse Coriolis parameter) is employed so that semi-geostrophic theory can quantitatively describe a number of subsynoptic scale phenomenon including the beginning of frontal collapse. Hoskins (1975) showed that by means of a suitable coordinate transformation (geostrophic coordinates) that the semi-geostrophic equations could be cast in the identical format to the quasi-geostrophic equations with two crucial differences. First the full absolute vorticity was retained in the divergence term of the vorticity equation instead of a constant map averaged Coriolis parameter. Consequently, cyclone spin-up could be much more rapid in a convergent cyclonic environment in a semi-geostrophic atmosphere. Second, the static stability (a function of pressure only) in the quasi-geostrophic omega equation was replaced by the geostrophic potential vorticity in the semi-geostrophic omega equation. Vertical motions could then become intense on small scales in regions where the potential vorticity approached zero. As of yet diagnostic and operational experience with the semi-geostrophic equations has been limited. Bosart and Lin (1984), however, showed that the semi-geostrophic vertical motions were more concentrated and sloped in the vertical in comparison with the quasi-geostrophic values on the basis of a single case study.

A very recent dynamical development (of which you will hear much discussion this week) involves the concept of isentropic potential vorticity (Hoskins et al., 1985). The concept can go beyond simple quasi-geostrophic theory (depending upon the nature of the assumed global balance relationship) to deduce the wind and mass fields from a knowledge of the isentropic potential vorticity distribution. Cyclogenesis is favored in regions where a positive potential vorticity anomaly near the tropopause begins to overspread a region of enhanced potential temperature gradient near the bottom boundary.

4. CASE STUDIES

4.1 Eastern North American Cyclogenesis of March 1971

In early March of 1971 a case of exceptional cyclonic development took place along the east coast of North America. A developing cyclone over eastern North Carolina with a central pressure of 985 mb at 0600 GMT 4 March "exploded" into a 959 mb center over eastern Massachusetts by 1800 GMT 4 March 1971, representing a pressure fall of 26 mb in 12 h. Another noteworthy aspect of this storm was the pronounced out-of-phase relationship between the thermal and geopotential fields throughout the troposphere and lower stratosphere prior to and accompanying development.

Here we will emphasize two points. First, substantial height falls in the mid and upper troposphere associated with pronounced potential vorticity advection dominate the environment upstream of the deepening storm. Cold advection into the trough and subsidence act to deepen the trough and generate cyclonic

frontogenesis.

Semi-geostrophic theory (Eliassen,1948) and Hoskins, 1975) has quantitatively improved upon quasi-geostrophic theory by allowing for advection by the full wind instead of the geostrophic wind in the presence of flow curvature. A Lagrangian time scale (long compared to the inverse Coriolis parameter) is employed so that semi-geostrophic theory can quantitatively describe a number of subsynoptic scale phenomenon including the beginning of frontal collapse. Hoskins (1975) showed that by means of a suitable coordinate transformation (geostrophic coordinates) that the semi-geostrophic equations could be cast in the identical format to the quasi-geostrophic equations with two crucial differences. First the full absolute vorticity was retained in the divergence term of the vorticity equation instead of a constant map averaged Coriolis parameter. Consequently, cyclone spin-up could be much more rapid in a convergent cyclonic environment in a semi-geostrophic atmosphere. Second, the static stability (a function of pressure only) in the quasi-geostrophic omega equation was replaced by the geostrophic potential vorticity in the semi-geostrophic omega equation. Vertical motions could then become intense on small scales in regions where the potential vorticity approached zero. As of yet diagnostic and operational experience with the semi-geostrophic equations has been limited. Bosart and Lin (1984), however, showed that the semi-geostrophic vertical motions were more concentrated and sloped in the vertical in comparison with the quasi-geostrophic values on the basis of a single case study.

A very recent dynamical development (of which you will hear much discussion this week) involves the concept of isentropic potential vorticity (Hoskins et al., 1985). The concept can go beyond simple quasi-geostrophic theory (depending upon the nature of the assumed global balance relationship) to deduce the wind and mass fields from a knowledge of the isentropic potential vorticity distribution. Cyclogenesis is favored in regions where a positive potential vorticity anomaly near the tropopause begins to overspread a region of enhanced potential temperature gradient near the bottom boundary.

4. CASE STUDIES

4.1 Eastern North American Cyclogenesis of March 1971

In early March of 1971 a case of exceptional cyclonic development took place along the east coast of North America. A developing cyclone over eastern North Carolina with a central pressure of 985 mb at 0600 GMT 4 March "exploded" into a 959 mb center over eastern Massachusetts by 1800 GMT 4 March 1971, representing a pressure fall of 26 mb in 12 h. Another noteworthy aspect of this storm was the pronounced out-of-phase relationship between the thermal and geopotential fields throughout the troposphere and lower stratosphere prior to and accompanying development.

Here we will emphasize two points. First, substantial height falls in the mid and upper troposphere associated with pronounced potential vorticity advection dominate the environment upstream of the deepening storm. Cold advection into the trough and subsidence act to deepen the trough and generate cyclonic

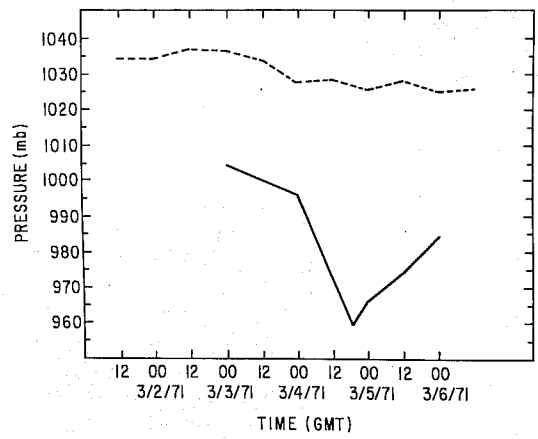

FIG. 1. Time series of central pressure (in millibars) of the cyclone (solid) and anticyclone (dashed).

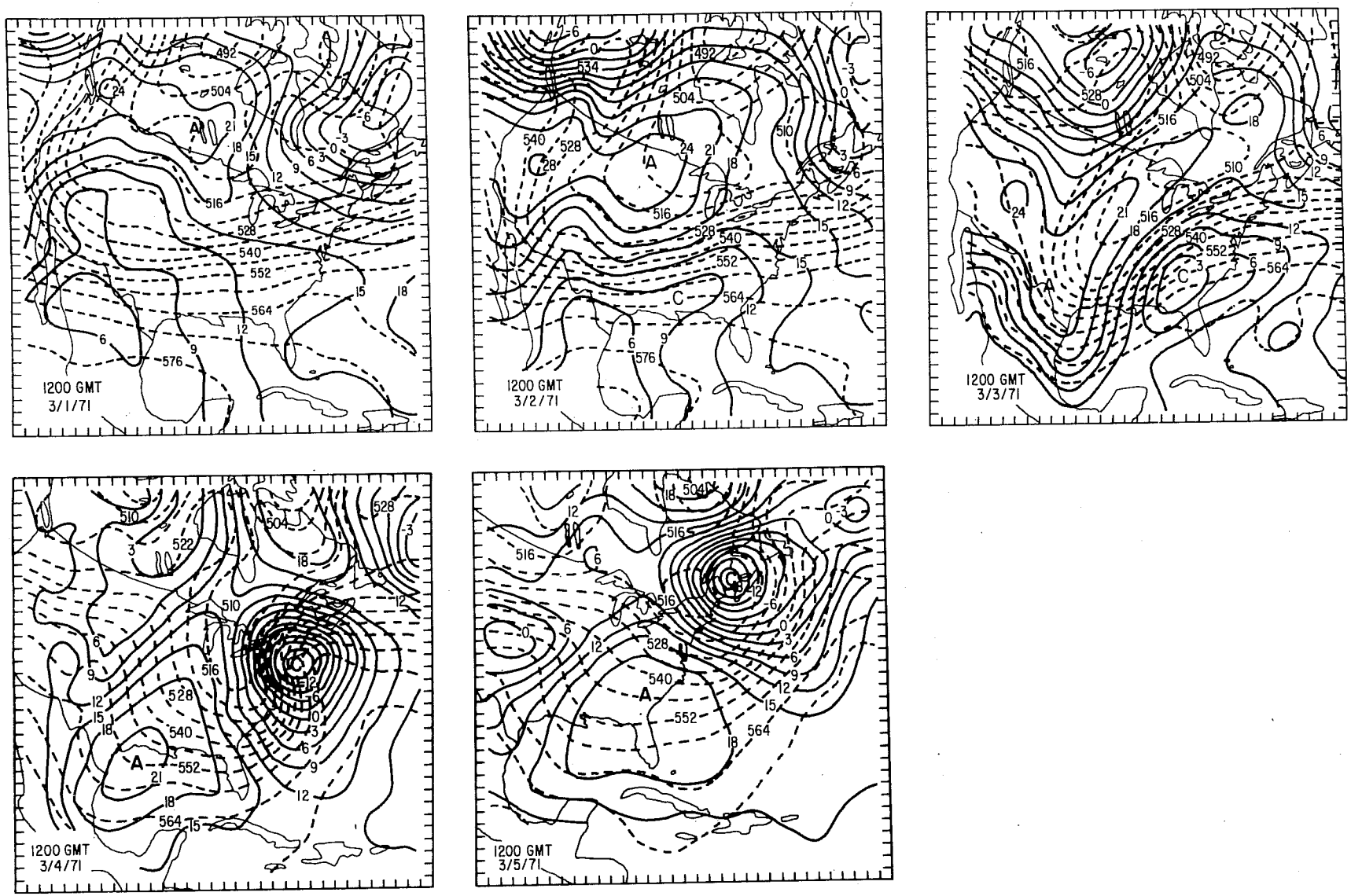

FIG. 2. 1000-mb heights (solid) and 1000 to 500 mb thickness (dashed) for times shown, (a)–(e), respectively. The height contour interval is 30 m, the thickness contour interval is 60 m. The tick marks along the edges of the plots indicate the gridpoint spacing. The cyclone center is marked with a C, anticyclone center with an A.

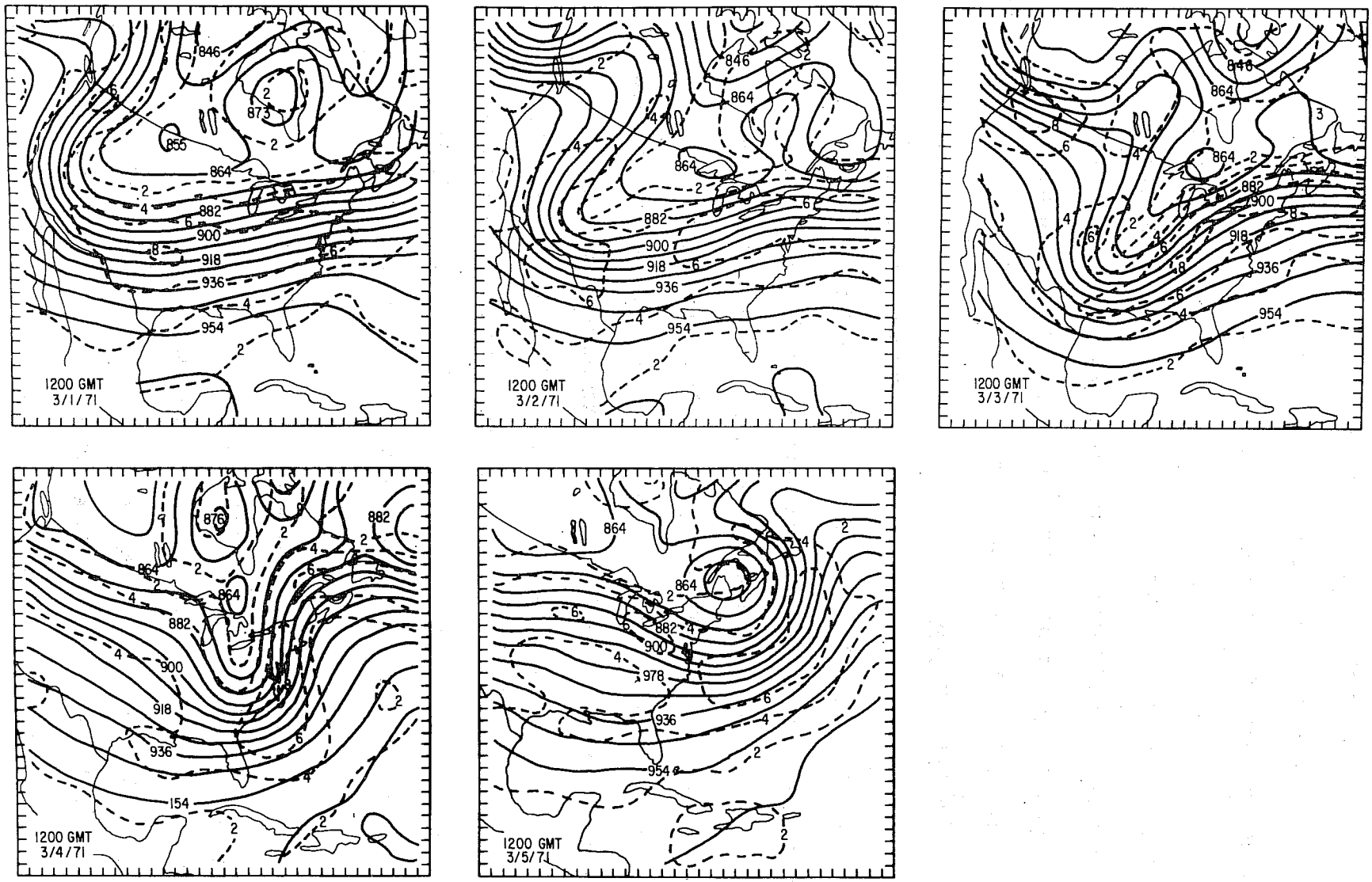

FIG. 3. As in Fig. 2 except for 300 mb heights (solid lines) and 300 mb isotachs (dashed lines). The height contour interval is 90 m, the isotach contour interval is 20 m s^{-1}.

vorticity which is then advected downstream over the deepening storm. Second, strong warm air advection in the upper troposphere overlies the surface storm during the period of most rapid intensification as the result of a sharply inclined tropopause. The tropopause is well defined from the potential vorticity field and in some cases it departs from the conventional lapse rate determined tropopause by more than 200 mb. A detailed analysis can be found in Boyle and Bosart (1986).

4.1a Synoptic Overview

A time series of the cyclone-anticyclone couplet central pressure is shown in Fig. 1. The anticyclone is long-lived and the central pressure is fairly steady expect for a 10 mb decrease during the 24 hour period ending 0000 GMT 4 March. The cyclone is first seen around 0000 GMT 3 March. Slow deepening in the presence of multiple centers ensues. This is followed by explosive development after 0000 GMT 4 March and then decay after 1800 GMT.

Figures 2 and 3 depict maps of the 1000 mb heights, 1000-500 mb thickness, and 300 mb heights and isotachs at 24 h intervals beginning 1200 GMT 1 March 1971. Initially, a broad baroclinic zone is in place along the west coast of the United States and then east-northeastward to New England. A frontal trough lies along the warm boundary of the baroclinic zone from Texas to the Carolinas. Twin anticyclone centers are found in southern Canada. Our interest will focus on the easternmost center just to the west of Lake Winnipeg. Aloft, a sharp 300 mb trough is moving southeastward through the southwestern United States. An upper tropospheric frontal zone is embedded in the northwesterly

flow behind this trough. By 1200 GMT 2 March a series of minor cyclonic impluses are propagating eastward along the frontal trough. A clear confluence line in the surface wind field (not shown) coincides with the trough. The thermal pattern at 500 mb (not shown) indicates cold advection into the trough, a sign of deepening.

By 1200 GMT 3 March, the 300 mb and 1000 mb troughs have both undergone substantial development. The thickness contours show a sharp thrust of cold air over the Western Gulf of Mexico ahead of the anticyclone which has weakened and moved rapidly southeastward into the Big Bend region of Texas. The cyclone located over Georgia initially formed on the warm side of the strong baroclinic zone over Louisiana around 1800 GMT 2 March. The upper level front is now located east of the trough aloft and the superposition of the upper and lower level fronts has resulted in a strong, deep baroclinic zone within which the cyclonic development proceeds. The upstream displacement of the 1000-500 mb thickness trough from the 500 mb geopotential trough ensures the advection of cyclonic vorticity by the thermal wind into the trough in accord with the development ideas of Sutcliffe (1947) and Trenberth (1978).

Rapid cyclonic development begins in the second half of the next period as the distance between the trough axis and downstream ridge line aloft shortens considerable. The surface cyclone's intense development and northeastward movement results in hurricane-like barograph traces in New England.

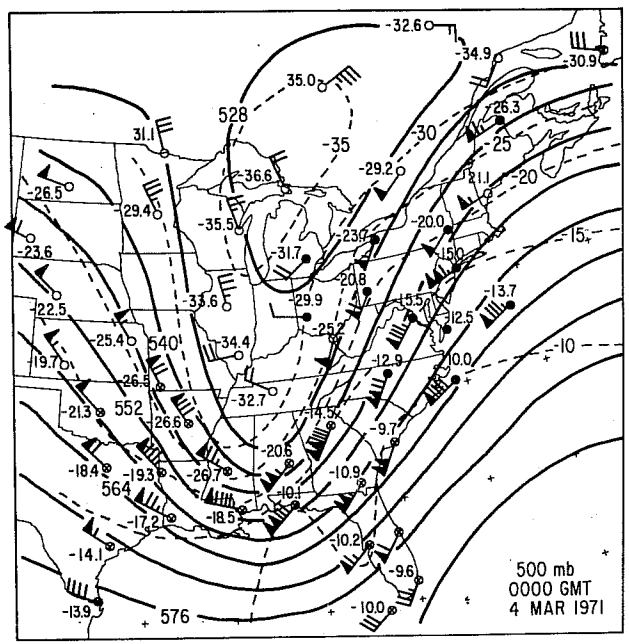

FIG. 4a. 500 mb sectional map valid 0000 GMT 4 March 1971. Geopotential heights (solid) every 6 dam; isotherms (dashed) every 5°C; relative humidity >70% (solid circles), between 30–70% (open circles) and <30% (crossed circles). Plotted winds in m s^{-1} with a pennant, full barb and half barb denote 25 m s^{-1}, 5 m s^{-1} and 2.5 m s^{-1} respectively.

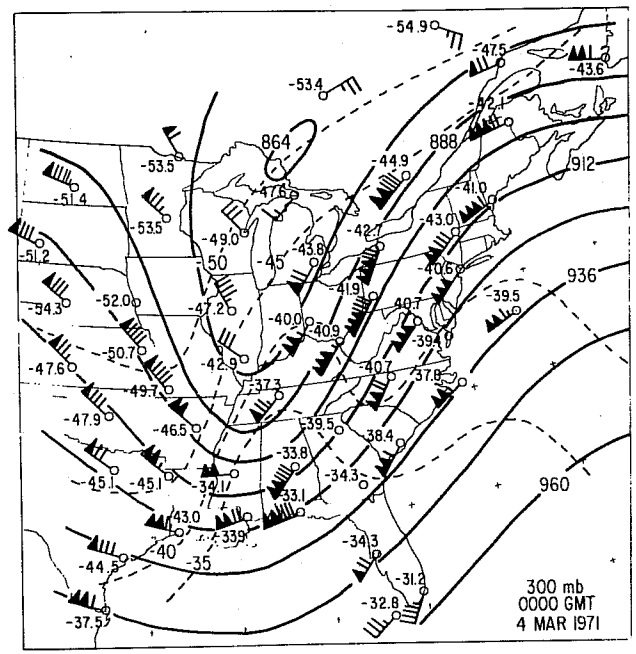

FIG. 4b. As in Fig. 4a except for 300 mb.

4.1b Upper Tropospheric Structure

Shown in Figs. 4a, b and 5a, b are 500 mb and 300 mb sectionals for 0000 and 1200 GMT 4 March. Particularly impressive is the cold advection into the trough at both levels. Downstream there is warm advection into the ridge region so that over the 12 h period the southerly flow aloft increases as the half-wavelength between the trough axis and downstream ridge line shortens. Coincident with this shortening the divergence aloft increases, the vertical motions become more vigorous and strong cyclogenesis ensues. At 300 mb the warm core nature of the trough increases by 1200 GMT 4 March with Cape Hatteras, North Carolina, recording a remarkably warm temperature of -28.1°C. Downstream of the warm 300 mb pocket at GMT 4 March there is exceptional warm advection overspreading the surface low center.

Figure 6 depicts the actual Cape Hatteras sounding. A frontal inversion between 850 and 700 mb marks the recent passage of the surface cold front. Cold advection is indicated by the backing winds in the lower half of the troposphere. A strong midtropospheric frontal region (and accompanying large vertical wind shear) is found between 600 and 500 mb. Above this level the wind speeds continue to increase rapidly with loss of signal just below 300 mb. Several stable laminae of the type described by Danielsen (1966) are embedded below the third major stable zone that extends to 285 mb. The highest stable layer lies deep in stratospheric air as will be demonstrated presently.

A vertical cross-section time series of potential temperature, wind speed, relative humidity, potential vorticity, and vertical motion for a 3X3 grid box centered on Cape Hatteras is

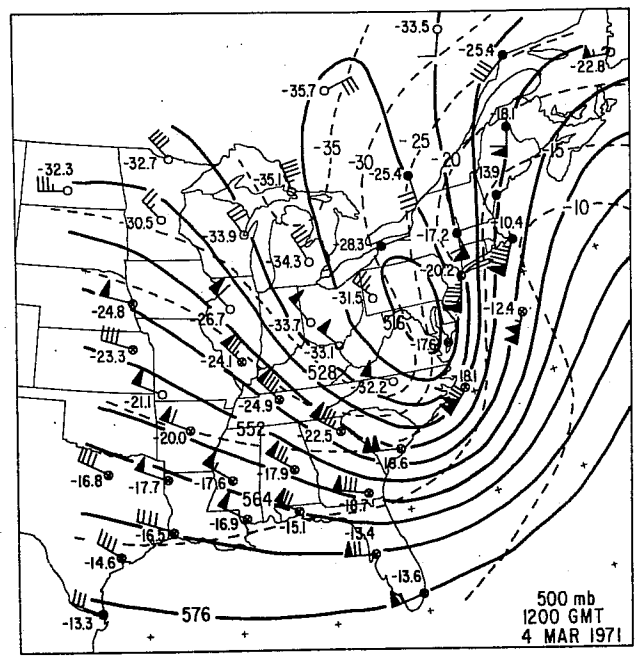

FIG. 5a. As in Fig. 4a except for 1200 GMT 4 March 1971.

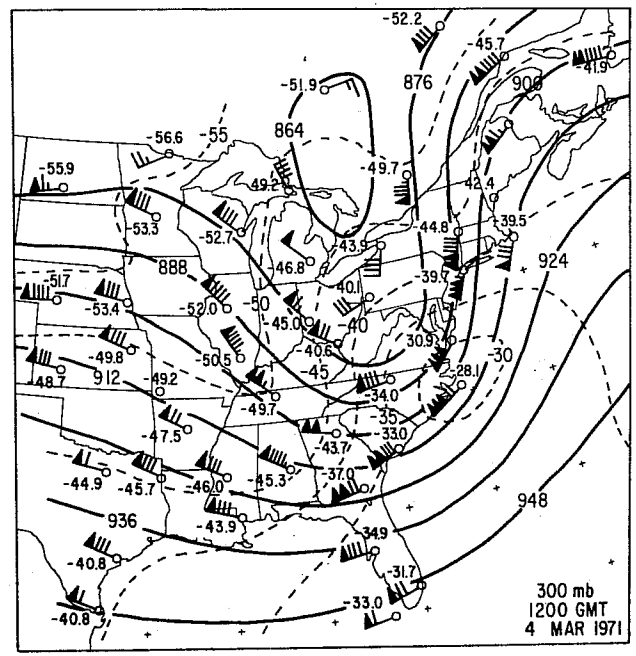

FIG. 5b. As in Fig. 4b except for 1200 GMT 4 March 1971.

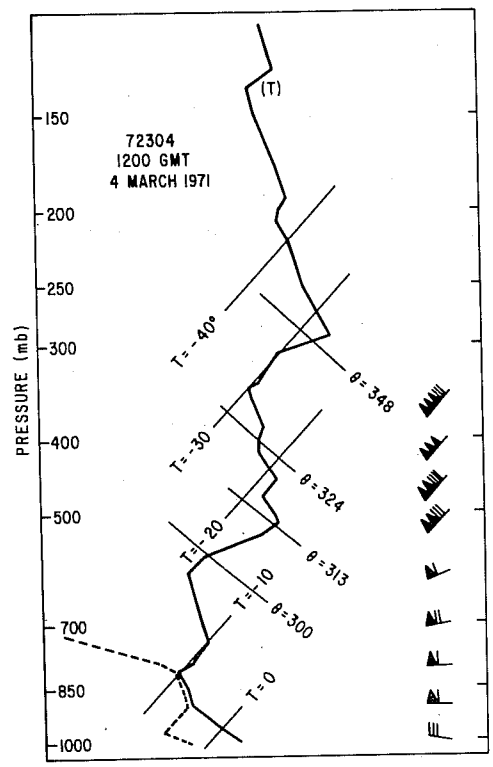

FIG. 6. Temperature (solid) and dewpoint (dashed) sounding (skew T–log p format) at Cape Hatteras, NC at 1200 GMT 4 March 1971. Plotted winds in m s^{-1} with a half barb, full barb and pennant denoting 2.5 m s^{-1}, 5 m s^{-1} and 25 m s^{-1} respectively.

shown in Fig. 7. There is strong cooling below 400 mb and warming above after 0000 GMT 4 March as the strong surface cold front passes the area. The gradients of relative humidity, wind speed, and vertical motion are strong with rapid and deep drying and a changeover from ascent to descent with frontal passage. Stratospheric values of potential vorticity (2×10^{-7} K kg^{-1} m^2 s^{-1} extend downward to almost 600 mb at 1200 GMT 4 March. The base of a stable layer near 600 mb in Fig. 6 is consistent with this interpretation whereas the reported tropopause at 138 mb is not. As will be remarked upon shortly, the conventional tropopause definition based upon lapse rate characteristics fails miserably in this case.

The trajectory method of Petersen and Uccellini (1979) was employed to trace the upstream origin of the 300 mb Cape Hatteras (HAT) air at 1200 GMT 4 March. A 12h θ = 348 K isentropic trajectory is shown in Fig. 8. It indicates that air parcels descended nearly 100 mb (average vertical motion of 2.2×10^{-3} mb s^{-1}) from a location near Fort Worth (FTW), Texas. The FTW 0000 GMT 4 March sounding (not shown) supports our assertion that the HAT air is of stratospheric origin near 200 mb 12h earlier.

Figure 9 outlines the region of stratospheric air enclosed by the 2×10^{-7} K kg^{-1} m^2 s^{-1} potential vorticity contour on the θ= 300 and θ = 324 K isentropic surfaces at 0000 GMT 4 March. The isobaric configuration of the stratospheric air shows that it penetrates below 600 mb along the Atlantic coast by 1200 GMT 4 March. Given this result additional 12h trajectories were

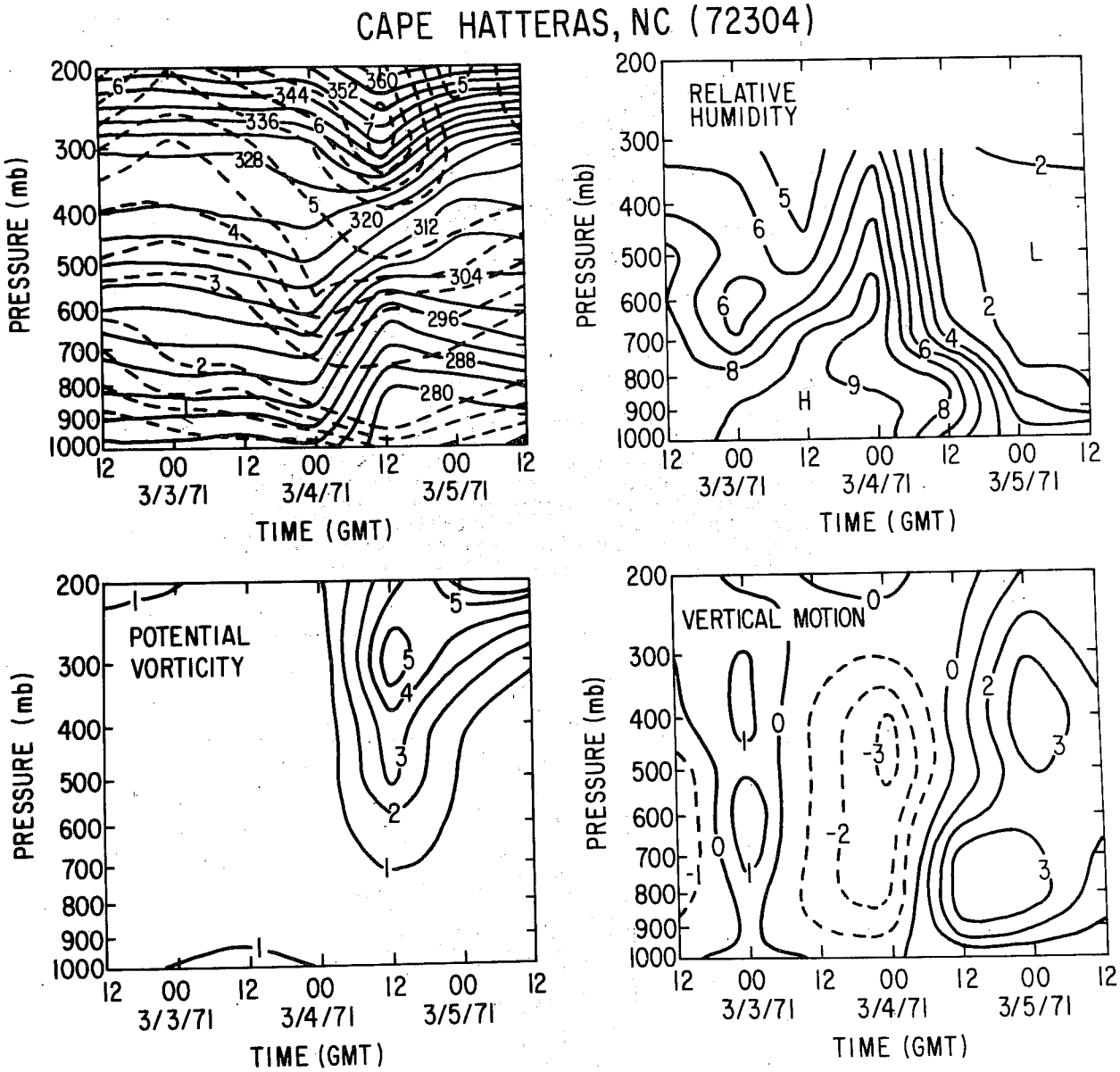

FIG. 7. (a) Upper left—Pressure-time series of potential temperature and wind speed averaged over a 3 × 3 point grid centered on Cape Hatteras, NC. Contour interval for potential temperature is 4 K. Contour interval for wind speed is 1×10^1 m s^{-1}. (b) Upper right—as in (a) except for relative humidity in percent. Contour interval is 10%. (c) Lower left—as in (a) except for potential vorticity. Contour interval is 1.0×10^{-7} K kg^{-1} m^2 s^{-1}. (d) Lower right—as in (a) except for the quasi-geostrophic vertical motion. Ascent (descent) indicated by dashed (solid) contours. Contour interval is 1.0×10^{-3} mb s^{-1}.

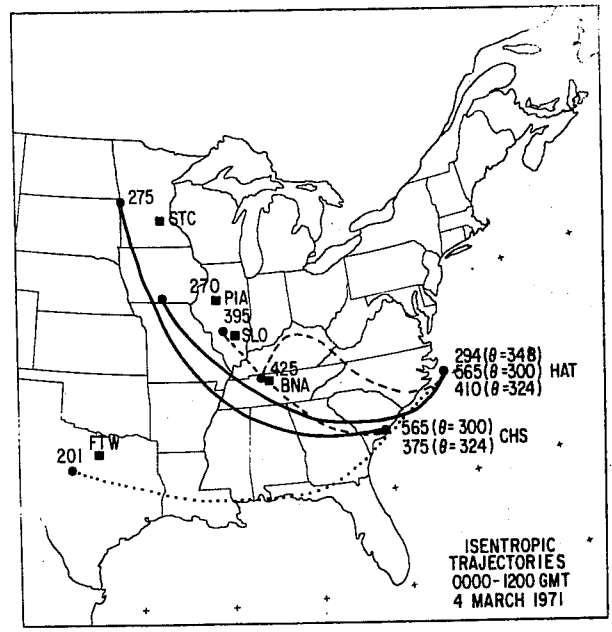

FIG. 8. 12-h isentropic trajectories ending at Cape Hatteras, NC (HAT) and Charleston, SC (CHS) at 1200 GMT 4 March 1971. Solid (dashed) lines denote trajectories on the $\theta = 324°K$ (300°K) surfaces. Beginning and ending pressures (mb) are plotted to the upper right of the trajectory beginning and ending points shown by solid circle. The dotted line represents a $\theta = 348°K$ trajectory (see text). Designators as follows: FTW (Forth Worth, TX), PIA (Peoria, IL). STC (St. Cloud, MN), SLO (Salem, IL) and BNA (Nashville, TN).

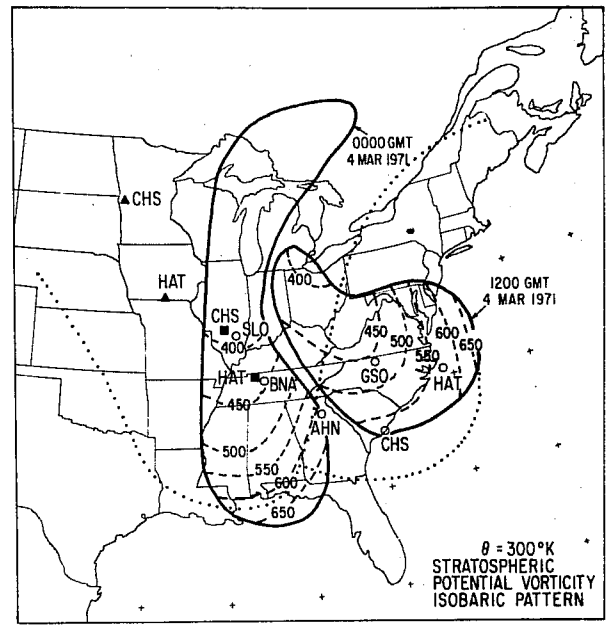

FIG. 9. Pressure (dashed, mb) configuration of stratospheric air enclosed by the 2×10^{-7} K kg^{-1} m^2 s^{-1} potential vorticity contour on the $\theta = 300°K$ isentropic surface at 0000 and 1200 GMT 4 March 1971. Dotted lines show outline of 2×10^{-7} kg^{-1} km^{-2} s^{-1} potential vorticity contour on the $\theta = 324°K$ isentropic surface for the same times. Solid squares and triangles indicate origin points for trajectories beginning on the $\theta = 300$ and 324°K surfaces respectively from Fig. 8. The three letter designators are as in Fig. 8 (also plotted next to trajectory origin point to indicate final location) except for GSO (Greensboro, NC).

constructed for air parcels terminating at HAT and Charleston (CHS), South Carolina, on the θ = 300 and θ = 324 K isentropic surfaces. These trajectories are shown in Fig. 8 and their points of origin are repeated in Fig. 9. These trajectories were constructed kinematically using the observed Montgomery stream function fields as 6h guidance from each map. The results shown in Figs. 8 and 9 clearly establish that air reaching the Carolina coast above θ = 300 K at 1200 GMT 4 March is of stratospheric origin through a deep layer and has subsided substantially over the 12h period (average value 5.5×10^{-3} mb s^{-1}). The computed potential vorticity at the origin and end points of the θ = 300 K and θ = 324 K trajectories is presented in Table 1.

TABLE 1. Potential vorticity at trajectory initial and final points

(Units: $\times 10^{-7}$ K kg $^{-1}$ m^2 s^{-1})

	Initial point	Final point
θ=300 K	BNA (5.0)	HAT (4.0)
	SLO (2.5)	CHS (2.5)
θ=324 K	STC (3.5)	CHS (3.5)
	PIA (5.0)	HAT (3.5)

We see that to within an error of 20-25% potential vorticity is conserved which lends further confidence to our finding of widespread stratospheric air in the midtroposphere. The tendency for potential vorticity to decrease for trajectories ending at HAT may reflect turbulent mixing along the axis of the strongest

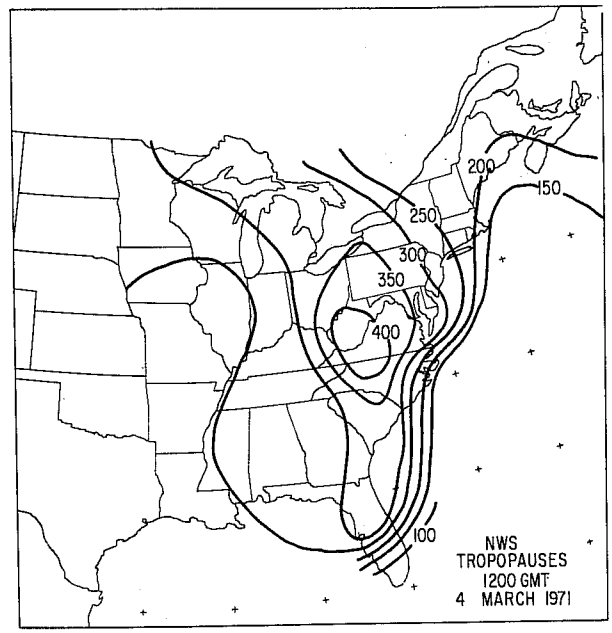

FIG. 10. Conventional tropopause pressures (mb) based on the National Weather Service reports for 1200 GMT 4 March 1971.

flow.

Figure 10 maps the isobaric configuation of the conventionally reported tropopause at 1200 GMT 4 March. Comparison with Fig. 9 shows major discrepancies with the pressure configuration of the stratospheric air on the θ = 300 K isentropic surface as determined from the field of potential vorticity. [For example, at HAT, the reported tropopause of 135 mb (Fig. 6) disagrees with the potential vorticity tropopause of 575 mb.] A tropopause analysis based upon the conventional definition will seriously underestimate the sloping nature of the tropopause in the vicinity of the mid- and upper tropospheric trough and toward the downstream ridge.

4.1c Potential Vorticity

Bleck (1974) described the evolution of potential vorticity and low level pressure patterns using a filtered model based on the advection of potential vorticity on isentropic surfaces. His Fig. 2 showed the link between the downward extrusion of high potential vorticity air of stratospheric origin and low level surface cyclogenesis. This extrusion of potential vorticity-rich air is an illustration of cyclonic vorticity generation by vortex tube stretching. This mechanism is the basis of the Kleinschmidt (1955) and Eliassen and Kleinschmidt (1957) theory of low level cyclogenesis. Bleck points out that the stretching required for cyclogenesis is due to the coincidence of the upper level advection of potential vorticity on 0 surfaces over a region of low level warm advection. Thus, cyclogenesis takes place where a high potential vorticity air mass aloft approaches the warm

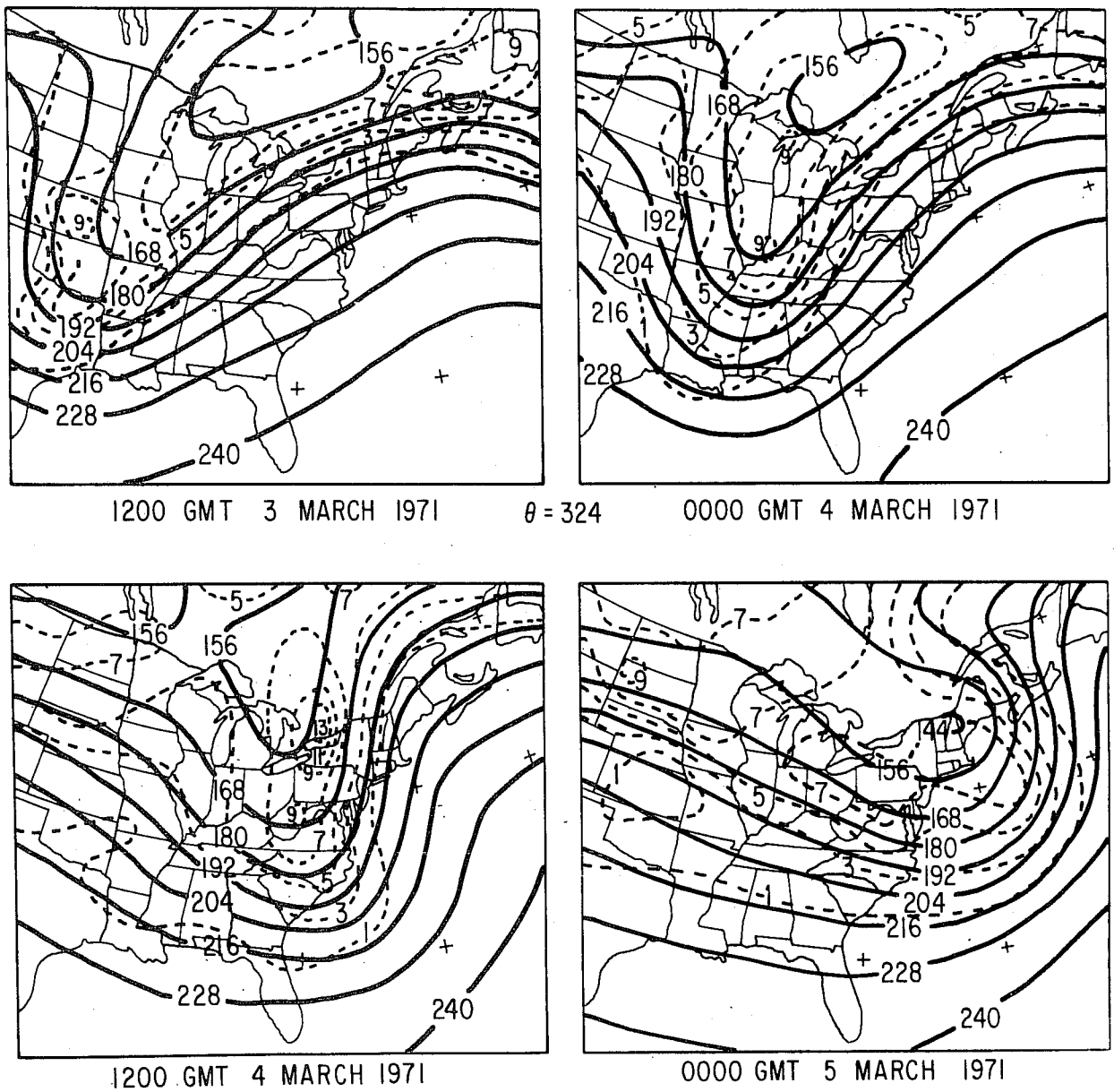

FIG. 11. Montgomery streamfunction (solid, contour interval 12×10^2 m^2 s^{-2}, leading 3 omitted) and potential vorticity (dashed, contour interval 2×10^{-7} K kg^{-1} m^2 s^{-1}) on the $\theta = 324$°K isentropic surface for the times shown.

southerly current near the surface. This yields a synthesis of the development theories of Sutcliffe (1947), Petterssen (1956), and Palmen and Newton (1969). The theoretical ideas in support of this assertion are elegantly summarized in Hoskins et al. (1985). Recently, Bleck and Mattocks (1984) have stressed the importance of quasi-geostrophic potential vorticity advection across the Alps as a precursor to Mediterranean Alpine lee cyclogenesis.

Figure 11 displays the Montgomery stream function field and potential vorticity structure on the θ = 324 K surface for the 36 h period ending 0000 GMT 5 March. Shown in Fig. 12 is the same Montgomery streamfunction field over which the isobaric configuration of the θ = 324 K surface and surface frontal positions are superposed. The θ = 324 K surface is representative of the layer of strong baroclinity between 500 and 300 mb. Together Figs. 11 and 12 make the following points: First, potential vorticity is a maximum above the cold dome of the trough. Second, potential vorticity advection is most pronounced along and to the east of the trough axis where the Montgomery streamfuction values are lowered in the following 12 h. Third, the potential vorticity advection tends to correlate well with cold advection into the trough and, fourth, the region of potential vorticity advection tends to lie upstream of the surface cyclone until well into the period of explosive development of the storm. A similar result is shown in Fig. 13 for the lower θ = 300 K isentropic surface. Figure 13 makes the further point that the out-of-phase relationship between the thermal wave and

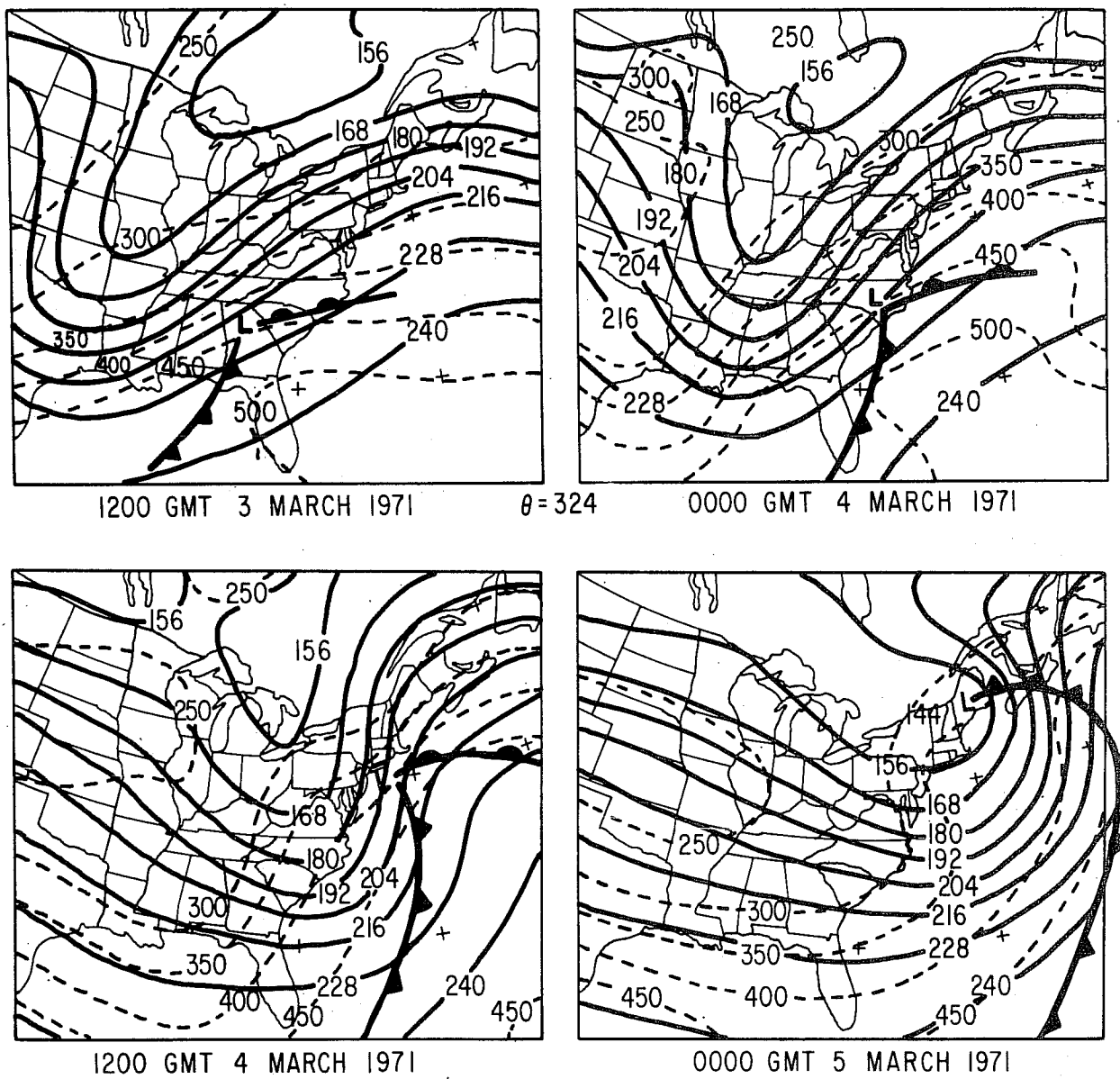

FIG. 12. As in Fig. 11 except pressure (dashed, mb) in place of potential vorticity.

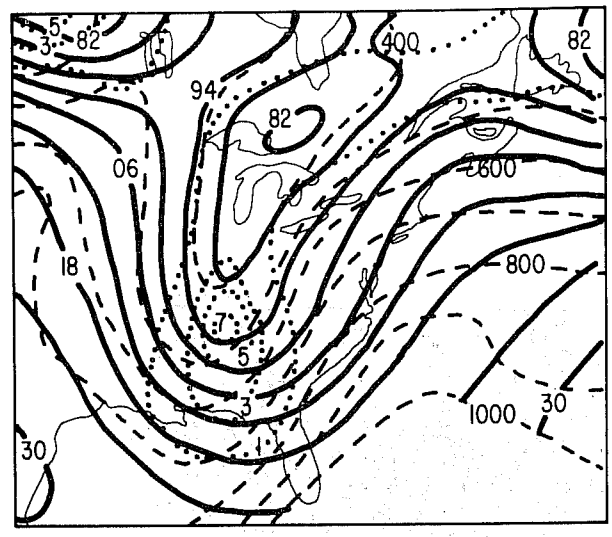

0000 GMT
4 MAR 1971

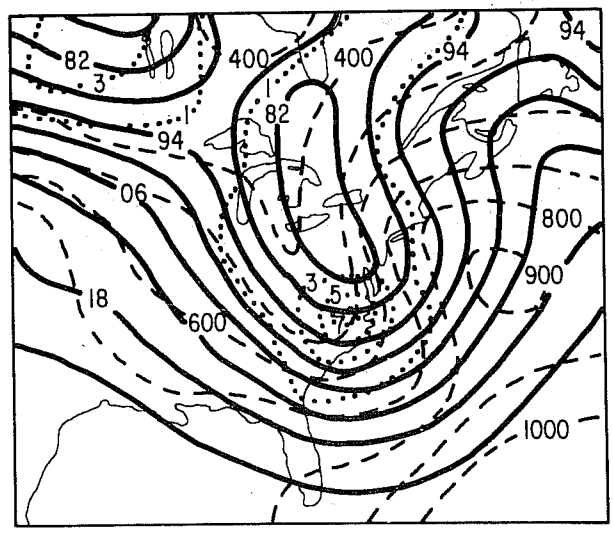

1200 GMT
4 MAR 1971

FIG. 13. Montgomery streamfunction (solid, contour interval 6 $\times 10^3$ m^2 s^{-2}, leading 2 or 3 omitted), pressure (dashed, mb) and potential vorticity (dotted, 10^{-7} K kg^{-1} m^2 s^{-1}) on the θ = 300°K isentropic surface for 0000 GMT 4 March 1971 (top) and 1200 GMT 4 March 1971 (bottom).

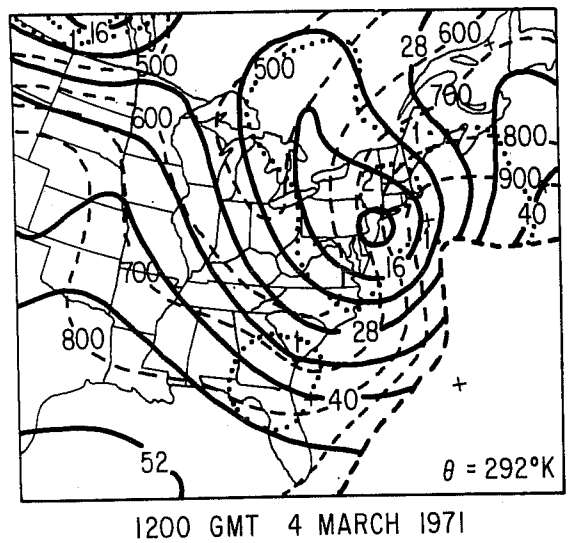

FIG. 14. Montgomery streamfunction (solid, contour interval 6 $\times 10^3$ m^2 s^{-2}, leading 2 omitted), pressure (dashed, mb) and potential vorticity (dotted, $\times 10^{-7}$ K kg^{-1} m^2 s^{-1}) on the $\theta = 292$°K isentropic surface for 1200 GMT 4 March 1971.

the Montgomery streamfunction wave enabled warm air advection to persist over New England and the Canadian Maritime Provences in the lower troposphere. On the average the pressures rose about 100 mb on the θ = 300 K surface in this region as the flow along the Atlantic coast became more southerly.

As cyclogenesis proceeds the potential vorticity maximum (PVM) overspreads the surface cyclone center from the southwest. As should be expected from previous work dealing with upper level fronts and high potential vorticity extrusions (e.g., see Danielsen, 1966; Mudrick, 1974; Reed and Sanders, 1955; Staley, 1960) the two are closely collocated. The picture of the potential vorticity extrusion and lower tropospheric cyclogenesis presented thus far is in agreement with the semigeostrophic model integrations of Heckley and Hoskins (1982). Their work shows that the upper tropospheric potential vorticity extrusion or tropopause fold develops back in the cold air to the southwest of the surface cyclone.

Finally, Fig. 14 presents the Montgomery streamfunction, pressure and potential vorticity on the θ = 292 K surface at 1200 GMT 4 March. A closed region of potential vorticity air in excess of 2×10^{-7} K kg^{-1} m^2 s^{-1} is located over southern and central New England and eastern New York. The high potential vorticity air is found just to the north of the closed cyclonic circulation center on the θ = 292 K surface and in a region of very strong warm advection over the 900-700 mb layer on this surface. Although the maximum potential vorticity values indicate "stratospheric" air by the aforementioned convention,

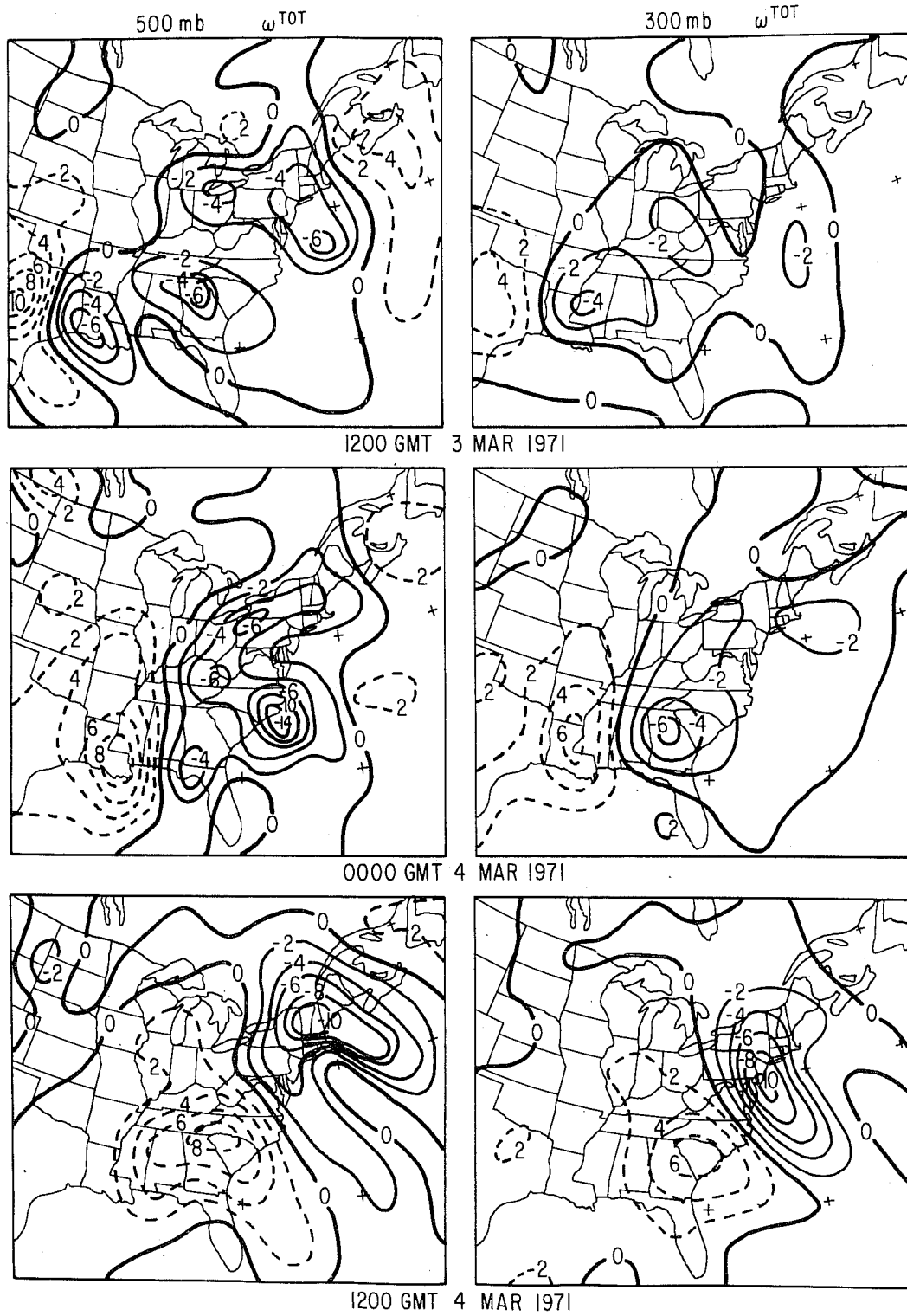

FIG. 15. Total quasi-geostrophic vertical motion ($\omega^V + \omega^T$ + stable latent heating term) for 500 mb (left) and 300 mb (right) at 1200 GMT 3 March 1971 (top), 0000 GMT 4 March 1971 (middle) and 1200 GMT 4 March 1971 (bottom). Units: $\times 10^3$ mb s^{-1} with ascent (descent) denoted by solid (dashed) contours.

the air in question is tropospheric with an origin near the surface. The potential vorticity maximum on the θ = 292°K surface does not have the temporal continuity (not shown) characteristic of the upper tropospheric potential vorticity maximum. While there is evidence for it at 0000 GMT 4 March, it is most strongly present 12 h later in Fig. 14. The potential vorticity maximum on the θ = 292 K surface in Fig. 14 appears to be generated by an upward increase of diabatic heating due to condensation. The region enclosed by the 2 X 10^{-7} K kg^{-1} m^2 s^{-1} isopleth has a maximum reported three hour precipitation of 6-12 mm for the period ending 1200 GMT 4 March. A similar, but less well defined, lower tropospheric potential vorticity maximum was found by Bosart and Lin (1984) and Uccellini et al. (1985) for the Presidents' Day storm of February 1979 and Gyakum (1983) for the QE-II storm.

4.1d Vertical Motion

Figure 15 shows the total quasi-geostrophic vertical motion at 500 and 300 mb for the 24 h period ending 1200 GMT 4 March. The total vertical motion consists of ω^V plus ω^T (differential vorticity advection and the laplacian of thermal advection) plus the contribution due to stable latent heating. Comparison of Figs. 4, 5, 11, 12, and 15 reveals that subsidence extends through the cold advection region to just east of the trough line at 500 and 300 mb. Greater subsidence is seen at 500 mb, so there will be vortex tube stretching and cyclonic vorticity generation in the 500-300 mb layer in the vicinity of the trough

axis. Immediately downstream of the area of cyclonic vorticity generation is the region of maximum positive potential vorticity advection and attendant geopotential height falls. In a Lagrangian perspective, as individual air parcels overtake the trough in the upper troposphere they must subside strongly (because of cold air advection) and develop cyclonic vorticity (because of vortex tube stretching). Testimony to the vigor of the subsidence is seen in the extraordinarily warm 300 mb temperatures along the coast of the Carolinas at 1200 GMT 4 March (We note with interest that Uccellini et al., 1985, and Reed and Albright, 1986, have emphasized the importance of strong subsidence in the mid- and upper troposphere into the trough region prior to the onset of major cyclogenesis.) The cyclonic vorticity so generated is advected rapidly downstream where it overspreads the surface cyclone. Because the downstream distance from the trough to ridge is shortening (recall Figs. 4 and 5) due to the large phase lag between the geopotential and isothermal fields above 500 mb, individual air parcels leaving the rapidly increasing cyclonic vorticity region in the heart of trough must rapidly lose this vorticity as they speed downstream toward the building ridge.

Figure 15 makes the further point that 300 mb ascent maximizes just ahead of the 300 mb trough axis whereas the 500 mb ascent pattern is more chaotic. There is a component of 500 mb ascent just ahead of the trough line at all three times. However, the maximum ascent at 500 mb at 0000 GMT 4 March is along the coast of North Carolina, largely due to diabatic heating, near the

developing storm center. Another area of 500 mb ascent is oriented along the central and northern Appalachian Mountains. By 1200 GMT 4 March one center of maximum ascent lies over northern New England with another (and more dubious) center to the southeast over the ocean. Stated another way the 300 mb ascent exceeds the 500 mb ascent immediately east of the trough line in this layer of the atmosphere. Consequently, vorticity generation by convergence is required through a deep layer, and there must be intense divergence above 300 mb. We conclude that with respect to an isobaric surface such as 400 mb the sloping level of nondivergence requires cyclonic vorticity generation immediately on both sides of the trough line. Large values of cyclonic vorticity are generated between 500 and 300 mb and are advected downstream. Farther downstream the level of nondivergence lowers to near 500 mb just ahead of the surface cyclone center where heavy precipitation is occurring. Therefore, vorticity-rich air parcels in the 500-300 mb layer encounter a transition from convergence to divergence and lose vorticity as they overspread the surface cyclone center while streaming northeastward.

In the lower troposphere there is vigorous ascent ahead of the rapidly deepening surface cyclone center, measured both quasi-geostrophically and via isentropic uplift across a very intense baroclinic zone. The equivalent of stratospheric potential vorticities are generated in the 900-700 mb layer centered on this ascent maximum.

4.1e Remarks

In summary, the March 1971 cyclogenetic event in eastern North America is noteworthy for the intensity of the surface development. It is hypothesized that the extraordinary deepening is a direct result of the pronounced thermal advection from the midtroposphere to the lower stratosphere across the trough axis toward the downstream ridge on the basis of the previous evidence. We can not say how the initial out-of-phase relationship between the thermal and geopotential trough is generated. We can say, however, that subsidence (and adiabatic warming) in the cold advection area leads to cyclonic vorticity generation in the trough. Very warm vorticity rich air is then advected downstream over the deepening surface cyclone center with consequent ridge development further downstream. The strongly sloping tropopause and potential vorticity advection is directly associated with the pronounced thermal advection pattern.

The upper tropospheric development follows the theoretical model of Heckley and Hoskins (1982) reasonable well with the exception that the potential vorticity extrusion is through a deeper layer and much more intense in conjunction with a steeply sloping tropopause in comparison to the model simulation. Eliassen and Kleinschmidt (1957) and Kleinschmidt (1955) interpret cyclogenesis in terms of the advection of "producing masses" (high potential vorticity air) across a baroclinic zone toward the warm boundary. Characteristically the isentropic surfaces bow upward (cold dome) beneath the high potential vorticity air as is observed in the March 1971 case.

Kleinschmidt (1955) presents an example of modest cyclogenesis in a strong baroclinic environment in which the potential vorticity maximum is presumed to lie well upstream of the surface cyclone. Unfortunately, given the considerable labor of the computation at that time, there is no direct evidence to support his assertion beyond a guess based upon geostrophic considerations. Hoskins et al. (1985) have quantified Kleinschmidt's ideas and provided several examples of how the process works from a global dataset. In the March 1971 development the area of positive potential vorticity advection only begins to overspread the surface cyclone at the time of rapid intensification. The role of strong positive potential vorticity advection is to force substantial height falls and cyclonic vorticity generation in the 500-300 mb layer across the upstream trough axis. From there the cyclonic vorticity is advected downstream and becomes an important factor in determining the vigor of the surface development. Figure 16 is an attempt to summarize these arguments in a schematic fashion.

Explosive cyclogenesis is a subject of considerable current research interest. Reed (elsewhere in this volume) has described the results of a numerical experiment performed by Y.-H. Kuo on the explosive eastern Pacific cyclone of November 1981 documented by Reed and Albright (1986). The mumerical simulations suggest that the rapid deepening arises from strong low-level ascent and associated large low-level condensation heating within a symmetrically neutral or unstable air mass. A notable characteristic of the Pacific storm was a very tight pressure gradient on a relatively small scale ($\sim$1000 km) resembling a

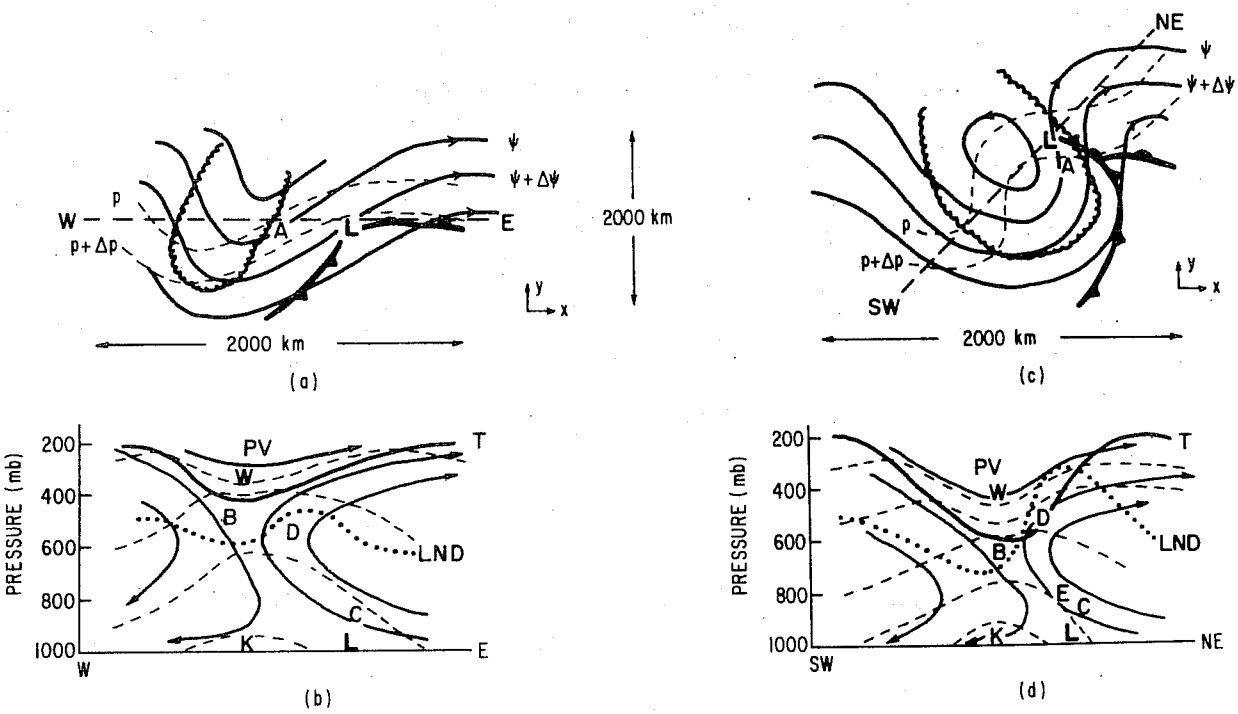

FIG. 16. Schematic diagram of major cyclogenesis associated with a sloping tropopause and level of nondivergence. (a) Isentropic upper tropospheric airflow accompanying incipient cyclogenesis. Confluent airstream denoted by Montgomery stream function contours (solid). Cold (warm) advection into trough (ridge) implied from isobaric (dashed) configuration. Positive potential vorticity advection is maximized at point A with stratospheric potential vorticity values outlined by escalloped line. (b) Vertical cross section of potential temperature (dashed) and airflow (solid lines) relative to the surface cyclone (L) in a plane along line W-E in (a). Stratospheric potential vorticity reservoir denoted by PV; sloping tropopause (heavy solid) and sloping level of nondivergence (heavy dotted) marked by T and LND respectively. Lower (upper) tropospheric cold (warm) air reservoir denoted by K (W). Ascending (descending) air will have a component into (out of) the cross section. B, C, D, E are described in the last paragraph. (c) As in (a) except for intense cyclogenesis phase after a closed vortex has developed aloft. (d) As in (b) except for intense cyclogenesis phase.

Positive potential vorticity advection lies well upstream of the developing surface cyclone during incipient cyclogenesis. The deepening mid- and upper tropospheric trough, and resulting cyclonic vorticity production, is forced by positive potential vorticity advection (deepening can also be deduced from the strong cold air advection into the trough). Downstream warm air advection helps to build the ridge. Together these thermal advection patterns oppose the powerful vorticity advection, acting to displace the entire pattern eastward. From a Lagrangian perspective individual air parcels must gain vorticity as they overtake the trough aloft and subside. Cyclonic vorticity is produced in region B by vortex tube stretching accompanying subsidence which maximizes at the LND. The vorticity so produced is advected downstream. Additional vorticity is generated in region D by horizontal convergence beneath the elevated LND upstream of the surface cyclone. Air parcels exiting the trough aloft must lose cyclonic vorticity rapidly by horizontal divergence which supports the development of a deep updraft and lower tropospheric warm air advection in locale C. Dynamically the sloping tropopause and lowered potential vorticity maximum allows a dome of cold air in the lower troposphere to remain vertically coupled with the potential vorticity maximum aloft. Surface cyclogenesis commences as the potential vorticity maximum aloft begins to cross the boundary of the cold air dome while moving toward warmer air.

During the intense cyclogenesis phase the tropopause and potential vorticity maximum lower to the midtroposphere. The tropopause and LND are strongly inclined. The high LND over the cyclone center ensures convergence and cyclonic vorticity generation through a deep layer accompanying the development of a cutoff vortex. Air parcels that gained vorticity by vortex tube stretching during subsidence in region B gain further vorticity by convergence above region C as they are advected downstream across the steeply inclined LND. (Note: our schematic is simplified to show one LND. It is possible that multiple LND's could exist.) The steeply inclined tropopause over the surface cyclone center results in appreciable warm air advection in the 400–200 mb layer which further contributes to the intensity of development. The resulting vertical circulation is very vigorous and warm air advection is maximized ahead of and just to the rear of the cyclone track in the inflow branch of this circulation. "Stratospheric" values of potential vorticity are generated in the lower troposphere at locale E beneath a region of maximum diabatic heating due to latent heat release.

"coiled spring" at the time of peak intensity. A similar coiled spring appearance characterized the Presidents' Day storm of February 1979 (Bosart, 1979; Bosart and Lin, 1984; Uccellini et al., 1984 and 1985). Explosive cyclogenesis resulted when a pronounced migratory short wave trough aloft overspread low-level vorticity rich and low static stability air. A low level ascent maximum was indicated. Similarly, Gyakum (1983) reported that a low static stability environment and convective latent heat release characterized the rapidly deepening phase of the QE-II storm. Uccellini (1986) offered an alternative interpretation that a pronounced jet aloft helped to trigger a deep vertical circulation prior to and accompanying the rapid cyclogenesis.

The March 1971 storm did not look like a small scale tight coiled spring development. Instead the baroclinicity throughout the troposphere was extreme. Cyclogenesis was triggered by a process that strongly resembled a type B storm (pre-existing upper level trough induces surface development) as described by Petterssen and Smebye (1971). Deep ascent was indicated throughout the troposphere and convection appeared to be of little consequence. It is suggested that explosive cyclogenesis is characterized by rather extraordinary baroclinic forcing in a low static stability environment. Tight small scale coiled springs appear to explode on time scales of 6h or less in vorticity rich low static stability environments. The maximum ascent is typically found in the lower troposphere ahead of an advancing potent short wave trough (positive isentropic potential vorticity anomaly) aloft.

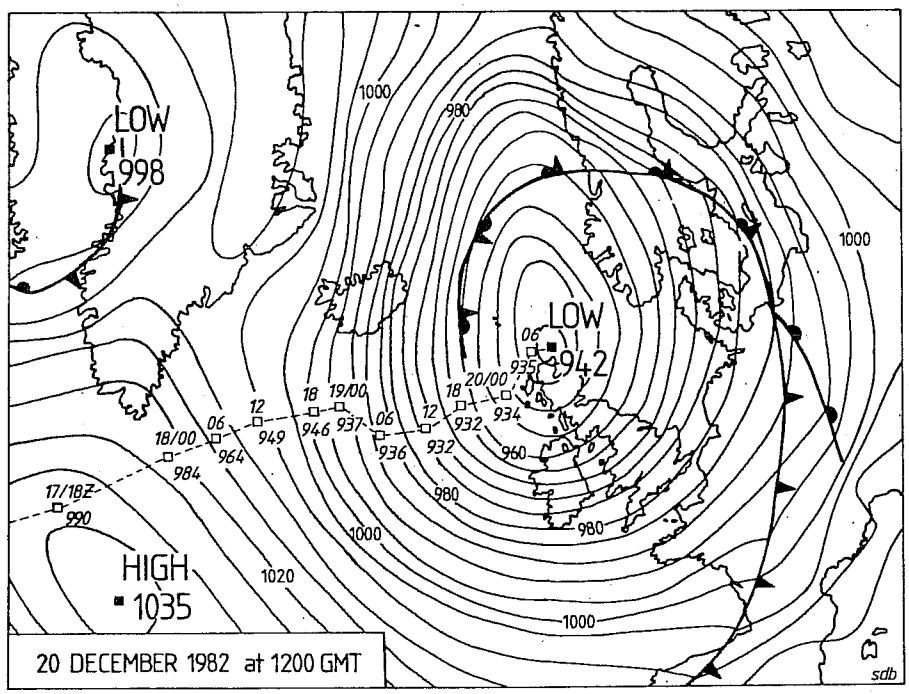

Fig. 17 Atlantic surface analysis at 1200 GMT on 20 December 1982, showing depression track and central pressure during the preceding 72 hours at six-hourly intervals. The isobars are drawn every 4 mbar

Source: Burt (1983)

4.2 North Atlantic Cyclogenesis of December 1982

Sanders (1987, personal communication and 1986a) and Hollingsworth (1987, personal communication) have stressed that operational prediction models at NMC and ECMWF have shown a dramatic improvement in their ability to predict explosively deepening cyclones or bombs of the type described by Sanders and and Gyakum (1980) and Sanders (1986b). A recent example is the intense depression of 17-20 December 1982 in the North Atlantic. Fig. 17, taken from Burt (1983), shows the surface features at 1200 GMT 20 December at which time a 942 mb central pressure cyclone was situated just north of the United Kingdom. The previous 72h history of the storm is also shown. Burt (1983) also noted that the British Meteorological Office operational prediction model simulated this storm very well.

The analyzed ECMWF 500 mb geopotential, thermal and wind fields for 1200 GMT 17 December and 0000 GMT 19 December are shown in figs. 18a, b respectively. At 1200 GMT 17 December a broad, flat ridge was located over the west-central Atlantic ocean upstream of a trough just west of the Greenwich meridian. Very fast westerlies ($\sim$75ms^{-1}) were found at jet stream level in the ridge. The trough associated with the storm development can be seen over extreme eastern Canada at 1200 GMT 17 December. Very cold air at 500 mb ($T < -40^{o}C$) was found in this trough. Frontogenesis (not shown) in the confluent flow ahead of the 500 mb trough contributed to the intensification of the mid tropospheric baroclinic zone and associated vertical wind shear.

By 36h later (fig 18b) the Canadian trough had raced

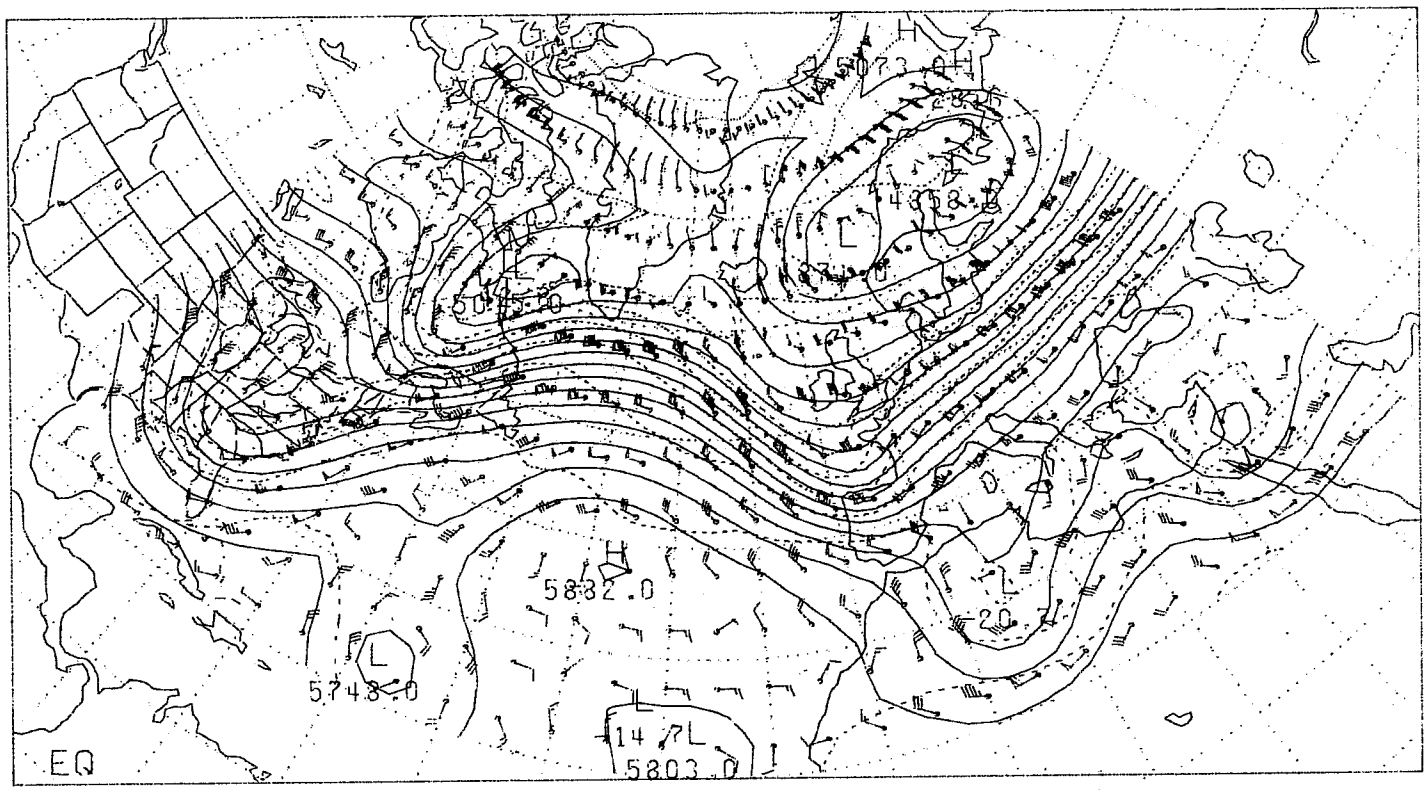

Fig. 18a. 500 mb heights (solid, dam), isotherms (dashed, °C) and winds (ms-1) for 1200 GMT 17 December 1982. Conventional plotting notation on winds with 1 pennant = 25 ms-1.

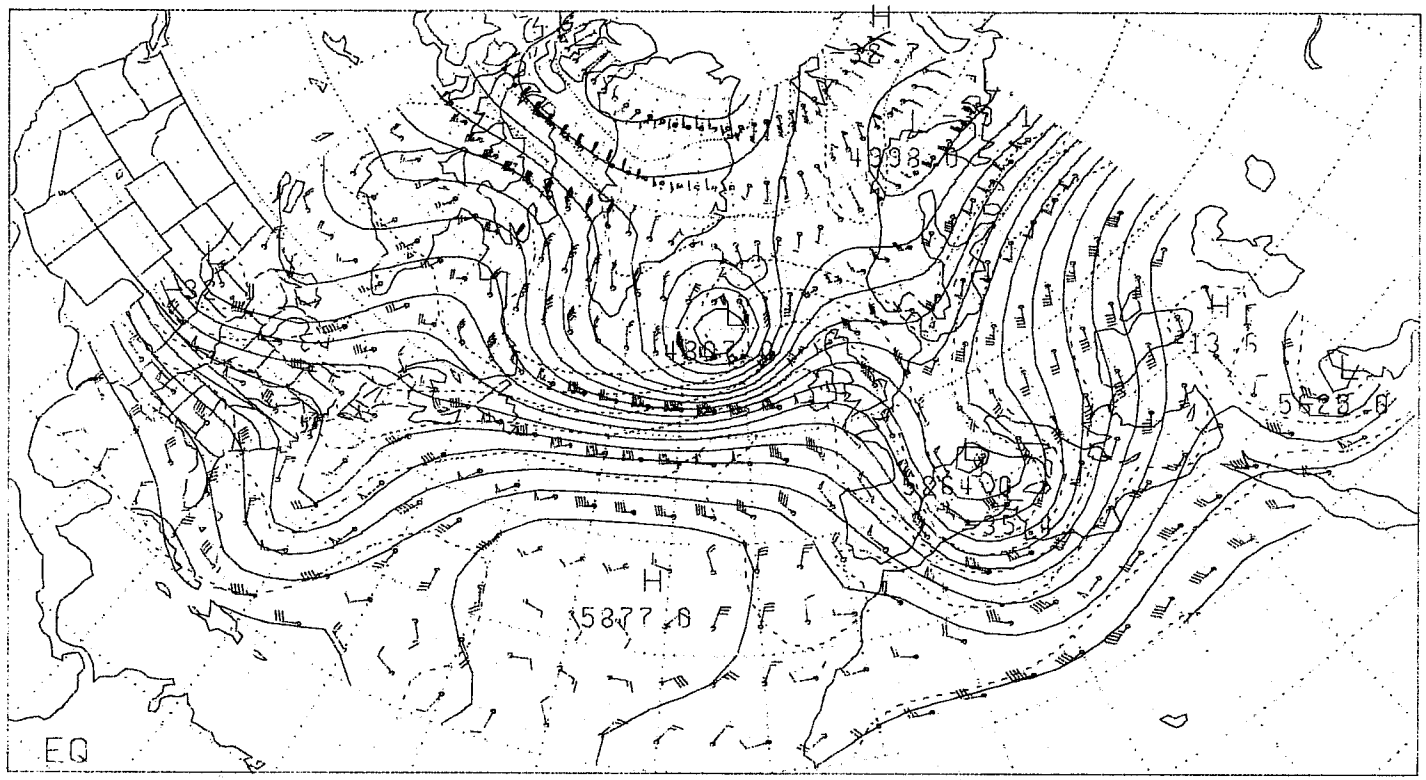

Fig. 18b. As in Fig. 18a except for 0000 GMT 19 December 1982.

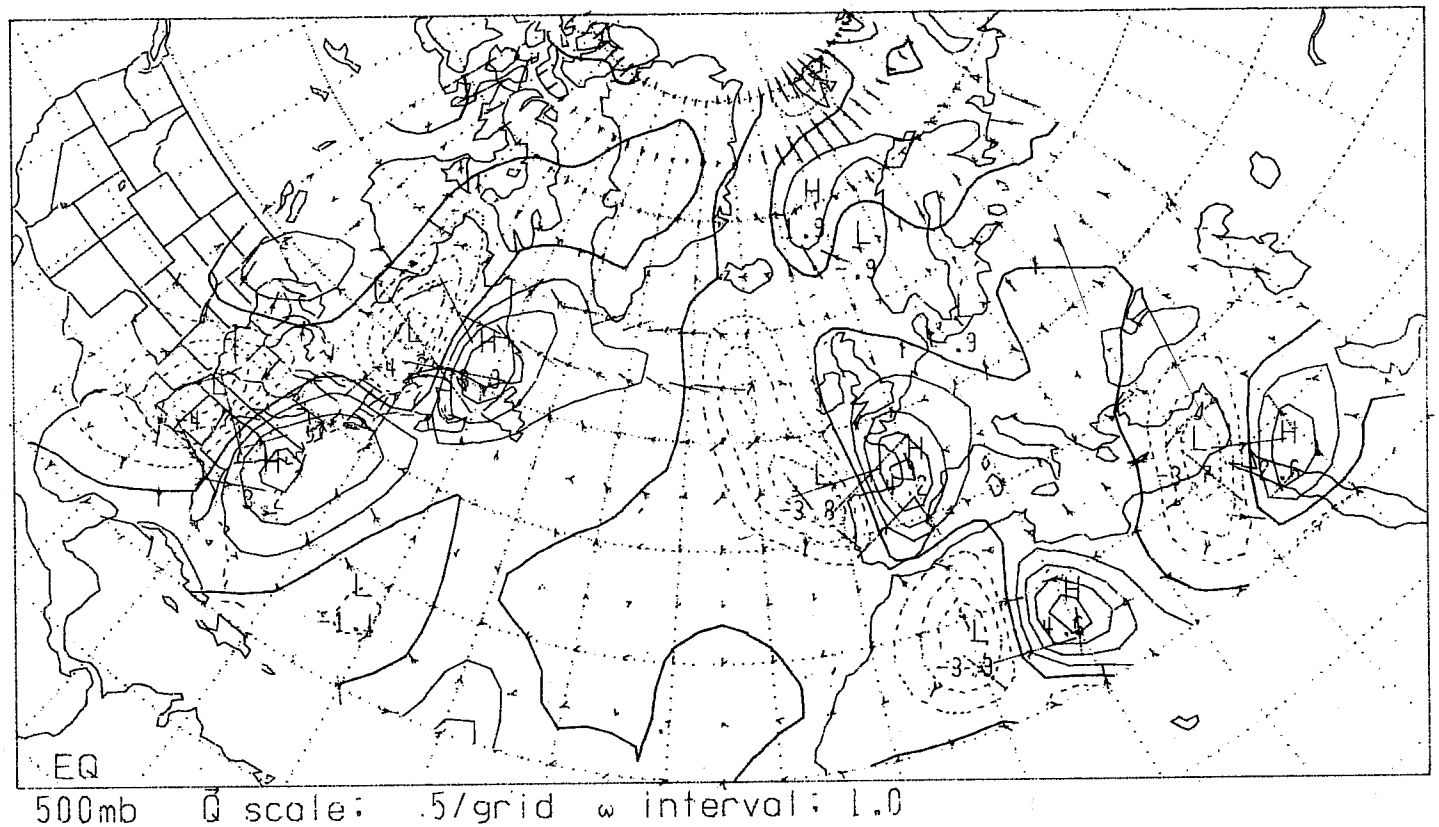

Fig. 19a. $\vec{Q}$-vector (X 10-10 ms-3 mb-1) and quasi-geostrophic omega (X 10-3 mb s-1) for 500 mb at 1200 GMT 17 December 1982. Ascending (descending) regions shown by solid (dashed) contours with zero contour heavy solid. Plotted $\vec{Q}$-vectors scaled as 0.5 X 10-1 ms-3 mb-1 for 2.5° latitude.

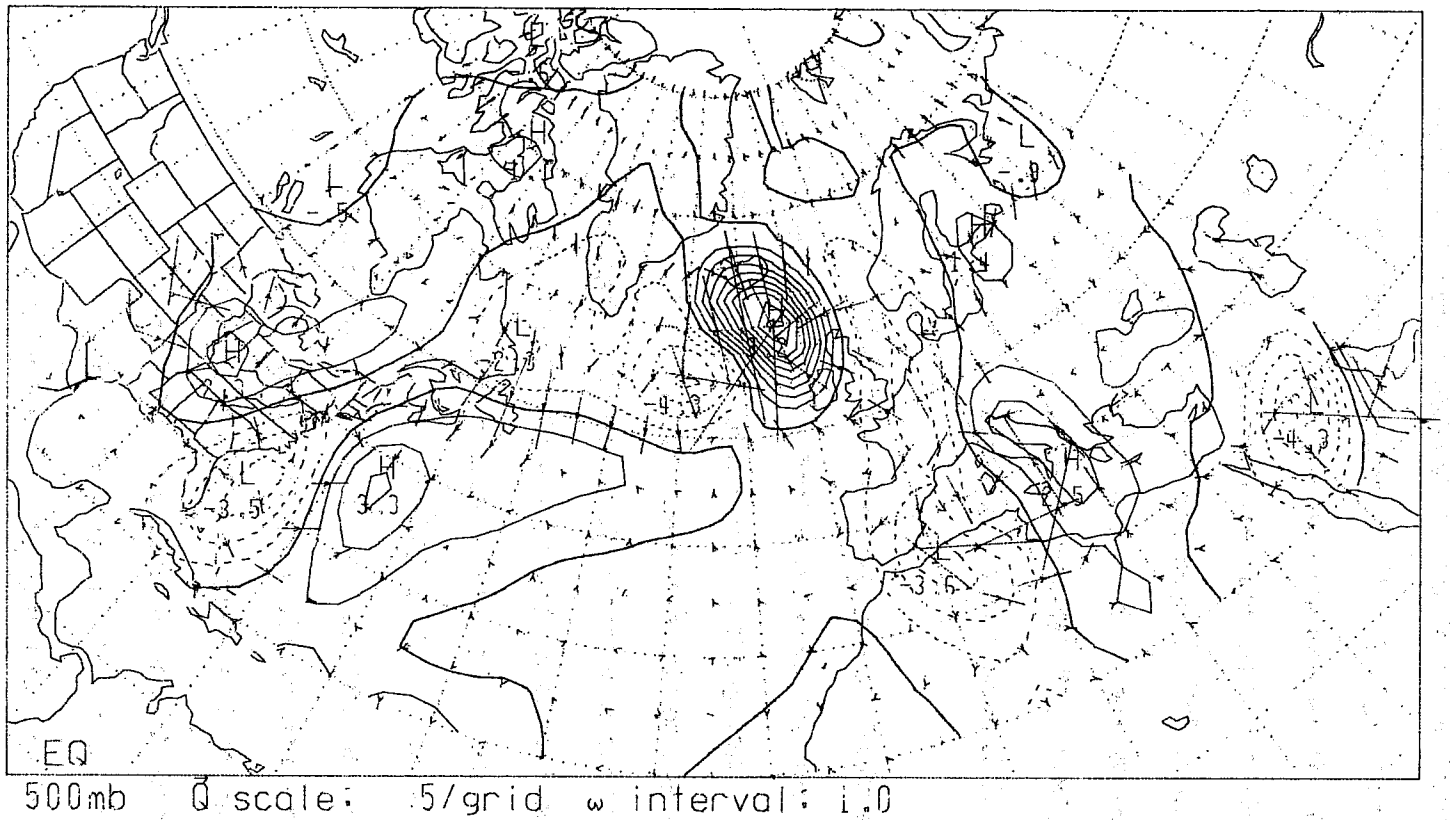

Fig. 19b. As is Fig. 19a except for 0000 GMT 19 December 1982

eastward to a location to the south of Iceland. An extremely strong westerly jet was created as the potent mobile short wave trough moved eastward north of the entrenched subtropical anti-cyclone. As seen from fig. 17 a 47 mb deepening over the 24h period ending 0000 GMT 19 December is indicated. Figs. 19a, b show the corresponding 500 mb quasi-geostrophic vertical motions and Q-vectors for 1200 GMT 17 December and 0000 GMT 19 December. These were computed by the method of Hoskins and Pedder (1980) from the gridded ECMWF 2.5° latitude-longitude analyses subject to the boundary condition of vanishing vertical motion at 1000 and 100 mb.

The 500 mb vertical motion pattern at 1200 GMT 17 December (fig. 19a) shows a typical ascent-descent couplet associated with synoptic scale cyclogenesis over extreme eastern Canada. A similar dipole pattern to the southwest along the east coast of the United States marks a separate slow moving trough that will have no direct impact on the explosive oceanic cyclogenesis. By 0000 GMT 19 December (fig. 19b) a respectable (considering the grid size) 500 mb ascent of -10×10^{-3} mb s^{-1} is concentrated on the eastern side of the intense 500 mb vortex. A cross section of potential temperature, vertical motion and meridional wind component at this same time along 10° W (fig. 20) reveals tropospheric deep ascent concentrated between 700-600 mb in a region of deep baroclinity. This vertical motion profile favors especially rapid cyclone spin-up because the horizontal convergence is concentrated relatively low ($\sim$700 mb) in the troposphere in a region where frontogenetical processes (not

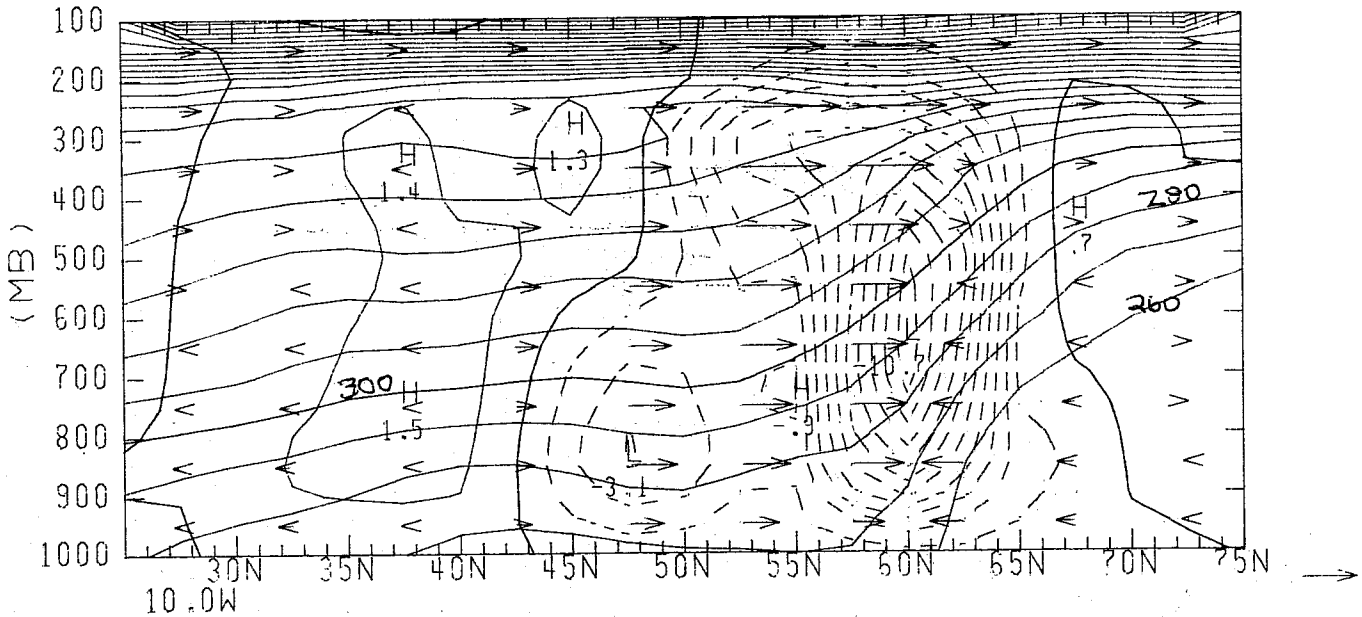

Fig. 20. Vertical cross section of potential temperature (solid), meridional wind component (arrows) and vertical motion (dashed or solid) along 10°W for 0000 GMT 19 December 1982. Isentropes every 10°K; ascent (dashed) and descent (solid) every 1 X 10-3 mbs-1 arrow; scale on lower right denotes 30 ms-1.

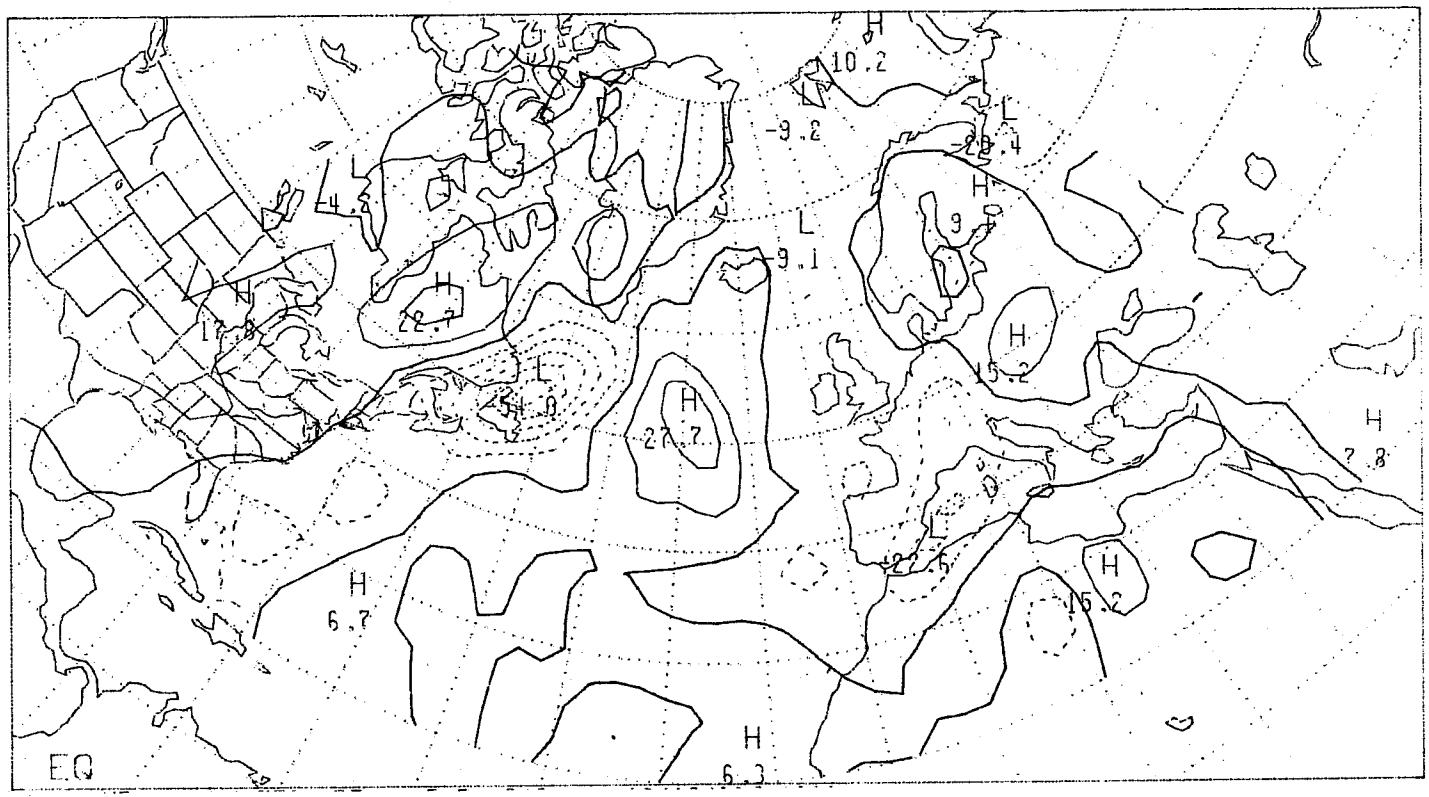

Fig. 21a. Potential temperature tendency (X 10-5 °C s-1) at 850 mb for 0000 GMT December 1982. Areas of warming (cooling) indicated by solid (dashed) contours.

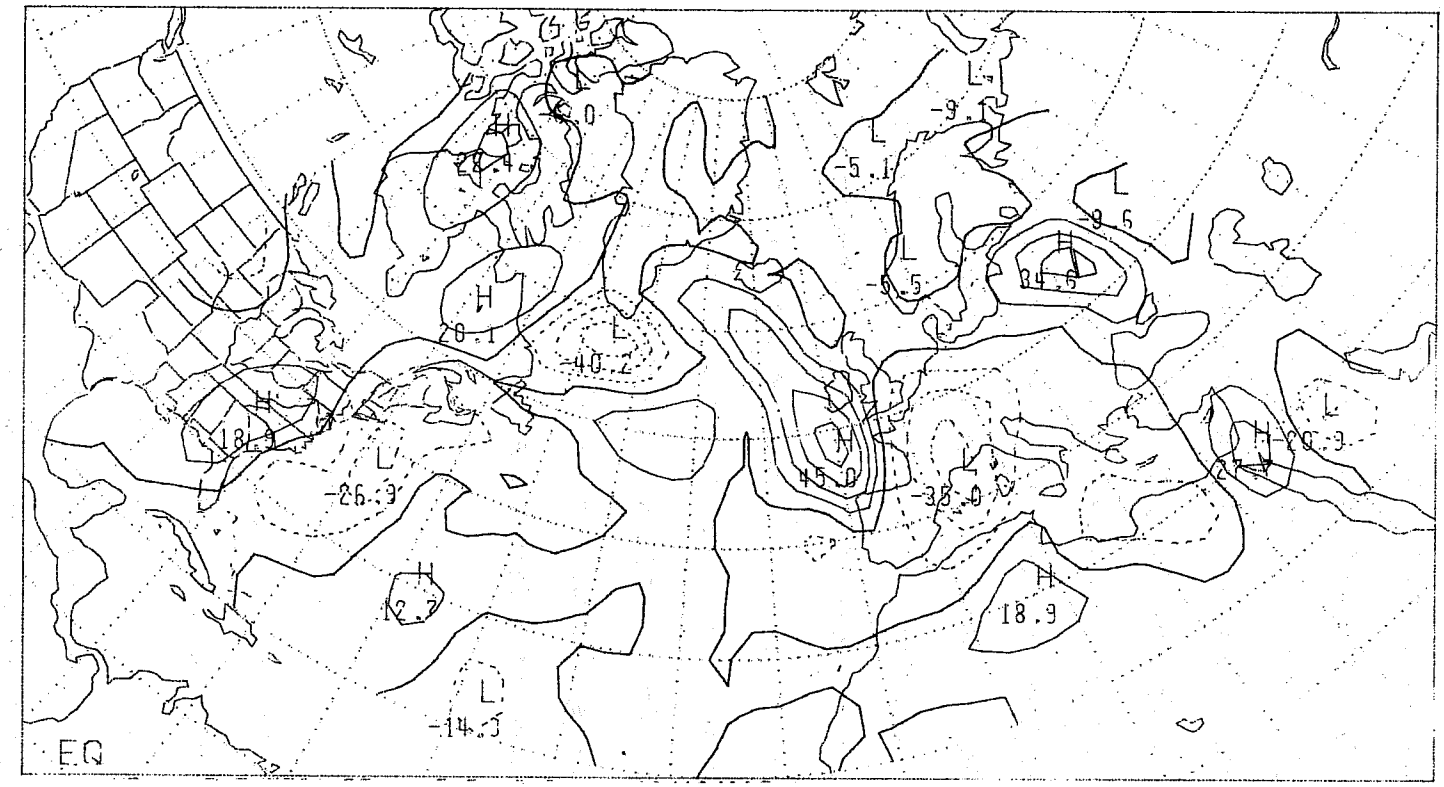

Fig. 21b. As in Fig. 21a except for 500 mb.

shown) are important in strengthening the horizontal temperature gradient.

Finally, fig. 21a, b shows the 850 mb and 500 mb local temperature tendency ($\partial\theta/\partial t$) computed as the sum of the horizontal and vertical advection of potential temperature ($-\vec{V}\cdot\nabla\theta - \omega\partial\theta/\partial p$) at 0000 GMT 18 December as explosive cyclogenesis began. Comparison with fig. 17 shows the surface low to be located just east of a region of maximum 500 mb cooling and along the changeover line from cooling to warming at 850 mb. The 500 mb pattern of $\partial\theta/\partial t$ favors a tightening of the temperature gradient with cooling and warming concentrated along the northern and southern boundary of the principal baroclinic zone. Meanwhile, the 850 mb pattern is more meridional with warming computed in advance of the cyclone and cooling to the rear. Taken together the 850 mb and 500 mb computed local potential temperature tendencies imply a destabilization of the lower tropospheric air mass immediately ahead of the surface cyclone.

In summary the explosive cyclone development of 17-20 December 1982 took place in a highly baroclinic environment in the presence of appreciable synoptic scale and frontogenetical scale forcing. There was no direct evidence for convection near the storm center at the outset of deepening although the reduction of the lower tropospheric static stability implied by synoptic scale differential thermal advection undoubtedly contributed to the increasing vigor of the ascent. Future research meeds to address the differences between larger scale

explosive events as typified by this case and the smaller scale (and less well forecast) "coiled spring" developments described earlier. This writer suspects the differences are more than just analysis or model resolution. Symmetric instability and convection may play an important role in the smaller scale "coiled spring" explosive cyclogenesis as noted by Reed (1987) elsewhere in this volume. Further support for this idea comes from the doctoral work of Rogers (1987) nearing completion.

Acknowledgement

The research of the author and his students has been supported by National Science Foundation grants ATM802655702, ATM8311106 and ATM8445006. The text was prepared by Celeste Iovinella.

5. References

Bleck, R., 1974: Short range prediction in isentropic coordinates with filtered and unfiltered numerical models. **Mon. Wea. Rev., 102**, 813-829.

------, R. and C. Mattocks, 1984: A preliminary analysis of the role of potential vorticity in alpine lee cyclogenesis. **Beitr. Phys. Atmos., 57**, 357-368.

Bosart, L.F., 1981: The Presidents' Day snowstorm of 18-19 February 1979: A subsynoptic-scale event. **Mon. Wea. Rev., 109**, 1542-1566.

------, 1985: Weather Forecasting. In: **Handbook of Meteorology**, D.D. Houghton, Editor-in-Chief, 205-279, John Wiley and Sons, 1461 pp.

------, and S.C. Lin, 1984: A diagnostic analysis of the Presidents' Day storm of February 1979. **Mon. Wea. Rev. 112**, 2148-2177.

Boyle, J.S. and L.F. Bosart, 1986: Cyclone-Anticyclone Couplets over North America. Part II: Analysis of a Major Cyclone Event over the Eastern United States. **Mon. Wea. Rev. 114**, 2432-2465.

Burt, S.D. 1983: New UK 20th Century low pressure extreme, **Weather, 38**, 209-211.

Charney, J.G., 1947: The dynamics of long waves in a baroclinic westerly current. **J. Meteor., 4**, 135-163.

Danielsen, E.F., 1966: Research in four-dimensional diagnosis of cyclonic storm cloud systems. Rep. No. 66-30, Air Force Cambridge Res. Lab., Bedford, MA, 53 pp. [NTIS AD-632668.]

Dole, R.M., 1987a: Persistent large-scale flow anomalies. Part I: Characteristics of developments. 1987 ECMWF Seminar Series: The Nature and Prediction of Extratropical Weather Systems.

------, 1987b: Persistent large-scale flow anomalies. Part II: Relationships to variations in synoptic-scale eddy activity and cyclogenesis. 1987 ECMWF Seminar Series: The Nature and Prediction of Extratropical Weather Systems.

Eady, E.T., 1949: Long waves and cyclone waves, **Tellus, 1**, 33-52.

Eliassen, A., 1948: The quasi-static equations of motion, **Geofys. Publ., 17**, No. 3.

------, 1984: Geostrophy. **Quart. J. Roy. Meteor, Soc., 110**, 1-12.

------, A. and E. Kleinschmidt, Jr. 1957: Dynamic meteorology. **Handbuch der Physik,** Vol. 58, Springer-Verlag, 1-154.

Gyakum, J.R., 1983: On the evolution of the QE II storm. I: Dynamic and thermodynamic structure. **Mon. Wea. Rev., 111,** 1156-1173

Heckley, W.A., and B.J. Hoskins, 1982: Baroclinic waves and frontogenesis in a non-uniform potential vorticity semi-geostrophic model. **J. Atmos. Sci., 39,** 1999-2016.

Holton, J.R., 1979: **An Introduction to Dynamic Meteorology,** Second ed., Academic Press, 319 pp.

Hoskins, B.J., 1975: The geostrophic momentum approximation and the semi-geostrophic equations, **J. Atmos. Sci., 32,** 233-242.

------, I.D. Draghici and H.C. Davies, 1978: A new look at the omega equation. **Quart J. Roy. Meteor. Soc., 104,** 31-38.

------, and M.A. Pedder, 1980: The diagnosis of middle latitude synoptic development. **Quart. J. Roy. Meteor. Soc., 106,** 707-719.

------, M.E. McIntyre and A. W. Robertson, 1985: On the use and significance of isentropic potential vorticity maps. **Quart. J. Roy. Meteor. Soc., 111,** 877-946.

Keshishian L., and L.F. Bosart, 1987: A case study of extended east coast frontogenesis. **Mon. Wea. Rev., 115,** 100-117.

Kleinschmidt, E., 1955: Die entstehund einer Hohenzyklone uber Nordamerika. **Tellus, 7,** 96-110.

Mudrick, S.E., 1974: A numerical study of frontogenesis. **J. Atmos. Sci., 31,** 869-892.

Palmen, E., and C.W. Newton, 1969: **Atmospheric Circulation Systems,,** Academic Press, 603 pp.

Petterssen, S., 1956: **Weather Analysis and Forecasting,** 2d ed., McGraw-Hill, 428 pp.

------, and S.J. Smebye, 1971: On the development of extratropical cyclones. **Quart. J. Roy. Meteor. Soc., 97,** 457-482.

Phillips, N.A., 1963: Geostrophic motion. **Rev. Geophys., 1,** 123-176.

Reed, R.J., 1987: Synoptic analysis and numerical modeling of an explosively deepening cyclone. 1987 ECMWF Seminar Series: The Nature and Prediction of Extratropical Weather Systems.

------, and M.D. Albright, 1986: A case study of explosive

cyclogenesis in the eastern Pacific. **Mon. Wea. Rev., 114**, 2305-2327.

------, and F. Sanders, 1955: An investigation of the development of a mid-tropospheric frontal zone and its associated vorticity field. **J. Meteor., 10**, 338-349.

Rogers, E., 1987: Case studies of explosive cyclogenesis, Ph.D. thesis, State University of New York at Albany, Department of Atmospheric Science, Albany, N. Y. 12222, USA (nearing completion)

Sanders, F., 1974: Quasi-geostrophic motions. Classroom notes. Dept. of Meteorology, Massachusetts Institute of technology, Cambridge, MA 02139, USA.

------, 1986a: Explosive cyclogenesis over the western North Atlantic Ocean, 1981-1984. Part II: Evaluation of LFM model performance. **Mon. Wea. Rev., 114**, 2207-2218.

------, 1986b: Explosive cyclogenesis over the western North Atlantic Ocean, 1981-1984. Part I: Composite structure and mean behavior. **Mon. Wea. Rev., 114**, 1781-1784.

------,and J.R. Gyakum, 1980: Synoptic dynamic climatology of the bomb. **Mon. Wea. Rev., 108**, 1589-1606.

Staley, D.O., 1960: Evaluation of potential-vorticity changes near the tropopause and the related vertical motions, vertical advection of vorticity, and transfer of radioactive debris from stratosphere to troposphere. **J. Meteor., 17**, 591-620.

Sutcliffe, R.C., 1939: Cyclonic and anticyclonic development. **Quart. J. Roy. Meteor. Soc., 65**, 518-524.

------, 1947: A contribution to the problem of development. **Quart J. Roy. Meteor. Soc., 73**, 370-383.

------, and A.G. Forsdyke, 1950: The theory and use of upper-air thickness patterns in forecasting. **Quart. J. Roy. Meteor. Soc., 76**, 1890-217.

Trenberth, K.E., 1978: On the interpretation of the diagnostic quasi-geostrophic omega equation. **Mon. Wea. Rev., 106**, 131-137.

Uccellini, L.W., 1986: The possible influence of upstream upper-level baroclinic processes on the development of the QE-II storm. **Mon. Wea. Rev., 114**, 1019-1027.

------, P.J. Kocin, R.A. Petersen, C.H. Wash and K.F. Brill, 1984: The Presidents' Day cyclone of 18-19 February 1979: Synoptic overview and analysis of the subtropical jet streak influencing

the pre-cyclogenetic period. **Mon. Wea. Rev., 112**, 31-55.

------, D. Keyser, K.F. Brill and C.H. Wash, 1985: The Presidents' Day cyclone of 18-19 February 1979: Influence of upstream trough amplification and associated tropopause folding on cyclogenesis. **Mon. Wea. Rev., 113**, 962-988.

Wallace, J.M. and M.L. Blackmon, 1983: Observations of low frequency atmospheric variability. In **Large Scale Dynamical Processes in the Atmosphere**, Edited by B.J. Hoskins and R.P. Pearch, **Academic Press**, 55-94

Figures

Note: Figures 1-16 are taken from Boyle and Bosart (1986)